UCLouvain

AGRO LOUVAIN

Faculté des bioingénieurs

Root system architecture of contrasted maize landraces under nitrogen deficit

Auteur : Emilie Devaux

Promoteurs : Pr. Xavier Draye (UCLouvain/ELIA)
Joséphine Guyot (UCLouvain/ELIA)

Lecteurs : Pr. Guillaume Lobet (UCLouvain/ELIA)
Pr. Christian Hermans (ULB/LPBP)

Année académique 2025-2026

Mémoire de fin d'études présenté en vue de l'obtention du diplôme de Bioingénieur : sciences agronomiques

Acknowledgements

Je tiens tout d'abord à remercier mon promoteur, le Professeur Xavier Draye, pour son accompagnement tout au long de cette année. Merci d'avoir toujours pris le temps de répondre à mes questions, de partager vos connaissances ainsi que vos réflexions, et de m'avoir guidée durant la réalisation de ce travail.

Je souhaite également remercier Joséphine , qui m'a intégrée à son projet de doctorat et m'a accompagnée tout au long de cette aventure. Merci pour tes conseils, tes remarques constructives et tes nombreux retours sur mon travail.

Je remercie sincèrement les membres de mon jury, le Professeur Guillaume Lobet et le Professeur Christian Hermans, d'avoir consacré du temps à la lecture et à l'évaluation de ce mémoire.

Un immense merci à Thomas pour tout le temps consacré à mes expériences. Merci de m'avoir transmis une partie de ton expertise sur cette fameuse plateforme, pour les nombreuses heures passées à résoudre les problèmes techniques, pour les discussions scientifiques comme plus personnelles, et pour avoir répondu avec patience à l'interminable série de questions que j'ai pu poser. Ta bonne humeur et ton enthousiasme ont largement contribué à rendre cette année plus agréable.

Je souhaite également remercier toutes les personnes qui m'ont aidée à différentes étapes des expérimentations. Merci à Marc et Romane pour leur aide lors des récoltes, ainsi qu'à Alice et Corentin pour leur participation aux mesures SPAD.

Je remercie l'ensemble du laboratoire PEPA pour l'ambiance chaleureuse qui y règne, les moments de convivialité partagés autour des puzzles, ainsi que l'intérêt et l'encouragement manifestés tout au long de l'avancement de ce mémoire.

Un grand merci également aux autres mémorants du laboratoire PEPA. Merci pour les échanges autour de nos projets respectifs, le soutien apporté durant les dernières semaines de rédaction, les conseils partagés, les discussions plus personnelles et tous les repas au resto u partagés.

Je tiens à remercier mes parents, qui m'ont soutenue et encouragée chacun à leur manière tout au long de mes études, et plus particulièrement durant cette dernière année consacrée à la réalisation de ce mémoire.

Enfin, je remercie les amis rencontrés au cours de mes études en bioingénierie pour toutes ces années partagées, ainsi que mes amis de plus longue date pour leur intérêt, leurs encouragements et leur soutien tout au long de ce parcours.

Contribution des auteurs et de l'intelligence artificielle

	Emilie Devaux	**Autres contributeur·rice**	**Intelligence artificielle**
Conceptualisation	X	Xavier Draye, Joséphine Guyot	
Méthodologie	X	Xavier Draye, Joséphine Guyot	
Investigation	X	Xavier Draye, Joséphine Guyot	
Analyse formelle	X	Xavier Draye, Joséphine Guyot	ChatGPT - code graphique
Validation	X		ChatGPT - reformulation
Rédaction – version originale	X		ChatGPT - reformulation, correction orthographe et grammaire
Rédaction – révision et édition	X	Xavier Draye, Joséphine Guyot	
Visualisation	X	Joséphine Guyot	ChatGPT - code graphique
Supervision		Xavier Draye, Joséphine Guyot	

Contents

List of Figures

List of Tables

Abbreviations

Abbreviation	Definition
AIC	Akaike's Information Criterion
DPD	Duration of primordium development
DW	Dry weight
EC	Electrical Conductivity
EMM	Estimated Marginal Means
FW	Fresh weight
LN	Low nitrogen
LR	Lateral root
LRBD	Lateral Root Branching Density
MLN	Moderate low nitrogen
N	Nitrogen
NUE	Nitrogen Use Efficiency
PC	Principal Component
PCA	Principal Component Analysis
PEPA	Plant Ecology, ecoPhysiology and sustainable Agriculture
RFID	Radio-Frequency Identification
ROI	Region of Interest
R:S	Root-to-Shoot Ratio
RSA	Root System Architecture
SR	Seminal root

1 Introduction

Nitrogen (N) is an essential element for plants and plays a central role in crop productivity and yield. Because N is often the most limiting nutrient for crop production, modern agriculture relies heavily on the application of synthetic N fertilizers to sustain high yields (Y. Wang et al., 2019; Yadav et al., 2017). Over the past decades, the use of inorganic fertilizers has increased markedly, reaching around 190 million tonnes worldwide in 2023 (FAO, 2025), illustrating the strong dependence of current agricultural systems on synthetic nutrient inputs.

Agriculture is recognized as one of the major sources of environmental pollution worldwide and N fertilization contributes substantially to these impacts. Plants generally absorb only 30 to 50% of the N supplied through fertilization, with N recovery often being even lower in irrigated systems than under rainfed conditions (Craswell, 2021; Yadav et al., 2017). The remaining N can be lost through several processes such as leaching, denitrification and volatilization (Cassman et al., 2002). These N losses contribute to major environmental and health issues, including groundwater contamination, eutrophication, biodiversity loss, soil acidification, atmospheric pollution and global warming through greenhouse gas emissions (Craswell, 2021). More broadly, the massive perturbation of the N cycle caused by agricultural fertilization is considered one of the planetary boundaries that has already been exceeded (Richardson et al., 2023). In addition, N fertilization contributes to several other planetary boundaries through its impacts on climate change, freshwater quality and biosphere integrity, highlighting the urgent need to improve N management in cropping systems (Steffen et al., 2015).

Beyond its environmental consequences, N fertilization also involves important economic and geopolitical challenges. The production of synthetic fertilizers is highly energy-demanding and strongly dependent on fossil fuels, particularly natural gas, both as feedstocks and energy sources (IPES-Food, 2025). Consequently, fertilizer prices are highly sensitive to fluctuations in energy markets and geopolitical tensions. Rising fertilizer costs increase production expenses for farmers, reduce profit margins and may ultimately threaten food affordability and farm sustainability (Blake, 2026).

In response to these environmental and economic challenges, there is growing interest in developing more sustainable and input-efficient agricultural systems. Approaches include improving N use efficiency (NUE), integrating organic nutrient sources and designing cropping systems that better match N supply with crop demand (Yadav et al., 2017; X. Zhang et al., 2015). Despite the development of these approaches, maintaining crop productivity while reducing N inputs remains a major challenge, since N availability strongly influences both crop yield and crop quality (Kandpal, 2021; Q. Wang et al., 2024).

2 State of art

N is an essential element for plant growth and development because it is involved in numerous metabolic, physiological and signalling processes. It is the fourth most abundant mineral element in plants after carbon, oxygen and hydrogen (Kochhar & Gujral, 2020) and plays a central role in plant metabolism (Mishra et al., 2024; Q. Wang et al., 2024). Plants mainly absorb N from the soil in inorganic forms, either as nitrate (NO_3^-) or ammonium (NH_4^+) (Zayed et al., 2023).

After uptake, nitrate is first reduced to nitrite (NO_2^- by nitrate reductase and then to ammonium by nitrite reductase (Figure 1). Ammonium is subsequently assimilated into amino acids through several enzymatic reactions (Q. Wang et al., 2024). Amino acids constitute the main form of N transport within the plant (Lalonde et al., 2004). Ultimately, N becomes incorporated into essential biomolecules such as proteins, nucleic acids, phospholipids, chlorophyll, hormones, vitamin and alkaloids (Q. Wang et al., 2024). Consequently, N is indispensable for photosynthesis, biomass production and overall plant development (Kochhar & Gujral, 2020; Zayed et al., 2023).

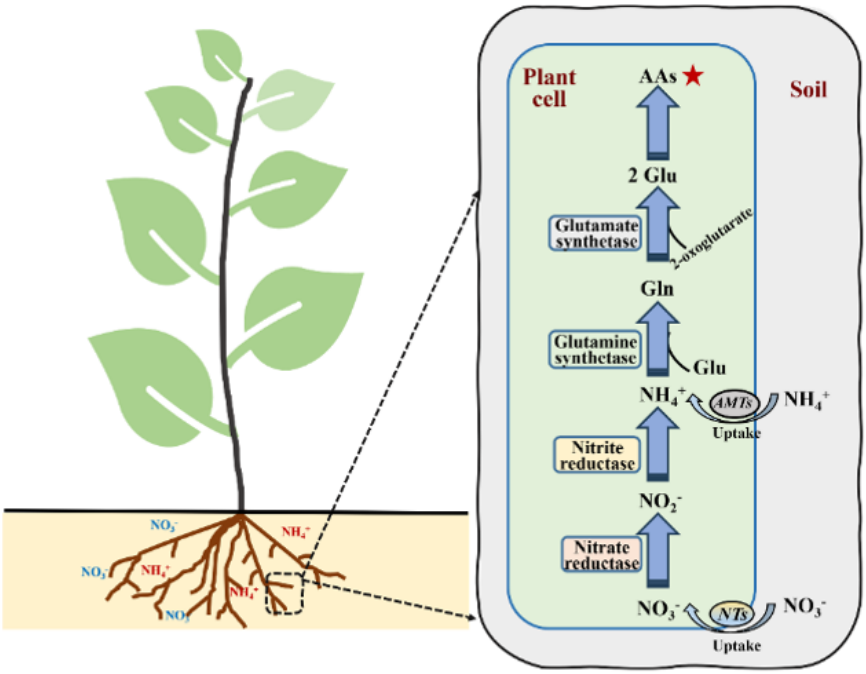

Figure 1: **Process of N assimilation in plants, from nitrate (NO_3^-) uptake to amino acid synthesis.** Nitrate is reduced into nitrite (NO_2^-) and subsequently into ammonium (NH_4^+), which is then assimilated into amino acids through enzymatic reactions involving glutamine synthetase and glutamate synthase (Q. Wang et al., 2024).

Beyond its structural and nutritional functions, N influences plant responses to environmental

conditions. Its availability regulates several signalling and stress-response pathways and influences the accumulation of protective compounds such as anthocyanins, which contribute to tolerance against both biotic and abiotic stresses (Q. Wang et al., 2024; J. Zhang et al., 2026).

2.1 Symptoms of Nitrogen stress

N deficiency induces major physiological and developmental changes in plants. Reduced N availability promotes leaf senescence and decreases photosynthetic activity, notably through the accumulation of sugars and starch in shoot tissues (Hermans et al., 2006; Wingler et al., 2006). At the same time, plants allocate proportionally more biomass to organs involved in resource acquisition, together with an increased translocation of sucrose toward the roots (Hermans et al., 2006). These adjustments generally result in an increased root-to-shoot (R:S) ratio under N-limited conditions.

N deficiency also strongly affects root system architecture (RSA), leading to important modifications in root growth and development (Hermans et al., 2006).

2.2 Nitrogen use efficiency

Most approaches proposed to improve the sustainability of agricultural systems ultimately aim to increase NUE, thereby maintaining crop productivity while reducing fertilizer inputs and environmental impacts (Congreves et al., 2021; Zayed et al., 2023). NUE is generally divided into two main components: N uptake efficiency, corresponding to the capacity of plants to acquire N from the soil and N utilization efficiency, referring to the efficiency with which absorbed N is converted into biomass or yield (Kochhar & Gujral, 2020).

Among these components, N uptake efficiency is particularly important under low N availability because it strongly depends on the ability of the root system to explore the soil and access spatially heterogeneous N resources. Consequently, RSA represents a major target for breeding programs aiming to improve NUE under reduced fertilizer inputs.

2.3 Constraints related to N availability

N availability in the soil is spatially and temporally variable. As said earlier, plants mainly absorb N as nitrate or ammonium, two forms that differ strongly in their behaviour within the soil profile. Nitrate is highly mobile because of its high solubility in water (Awasthi & Laxmi, 2021; Dathe et al., 2016; Dunbabin et al., 2003b), whereas ammonium is less mobile since it can be retained on cation exchange sites in the soil. However, ammonium is frequently converted into nitrate through microbial nitrification processes (Cassman et al., 2002).

Because of these transformations and of nitrate mobility, N can be present both near the topsoil and in deeper soil layers. Its availability is further influenced by microbial mineralization processes, which are themselves affected by environmental conditions such as temperature and soil moisture (J. P. Lynch et al., 2024).

N acquisition is also influenced by interactions between neighbouring plants. In dense plantings, competition for N becomes stronger, reducing N availability at the individual plant level (J. P. Lynch, 2013; J. P. Lynch et al., 2024). Because N distribution in the soil is highly heterogeneous and continuously changing, plants rely strongly on RSA to optimize N foraging and uptake.

2.4 Root system architecture and root functions

RSA refers to the spatial configuration of the root system, corresponding to the geometric deployment of root axes in the soil (J. Lynch, 1995). Studies of RSA generally focus on the organization of the entire root system or on large subsets of roots rather than on fine anatomical structures such as root hairs (J. Lynch, 1995). As such, RSA describes how roots are distributed in time and space within the soil environment and therefore determines the spatiotemporal pattern of soil exploration by the plant (J. P. Lynch, 2022).

Root systems play a central role in plant productivity because they ensure plant anchorage and the acquisition of water and mineral nutrients required for growth and development (Dunbabin et al., 2003a; Hochholdinger & Zimmermann, 2008). Since these resources are heterogeneously distributed throughout the soil profile, the spatial deployment of roots strongly influences their acquisition (J. Lynch, 1995). The RSA therefore sets an upper limit to the ability of plants to exploit soil resources efficiently (Hirel et al., 2007; J. Lynch, 1995; J. P. Lynch, 2013; Schneider et al., 2022). For example, phosphorus is relatively immobile and remains concentrated near the root surface, whereas nitrate is highly mobile and can move through the soil profile with water, requiring root systems capable of exploring different soil domains (Dunbabin et al., 2003a).

Root architectures differ greatly among plant species and environments, suggesting strong interactions between root development and adaptation to local soil conditions (Dunbabin et al., 2003b). Different soil environments may therefore favour distinct root foraging strategies, resulting in a wide diversity of root morphologies and architectural organizations throughout the plant kingdom (Dunbabin et al., 2003b; Fitter et al., 1991). This diversity reflects the existence of multiple adaptive solutions for soil exploration and resource acquisition depending on the environmental context and the spatial and temporal distribution of resources (Dunbabin et al., 2003b).

Plant root systems are composed of several classes of roots differing in origin and function. Based on their organ of origin, at least four major classes of roots can be distinguished: roots originating from the seed, the shoot, the hypocotyl or mesocotyl and lateral roots (LRs) originating from other roots (Postma et al., 2014; Zobel & Waisel, 2010). LRs generally represent most of the

total root length, although not necessarily most of the root biomass because of their smaller diameter (Postma et al., 2014). The organization of these different root classes, together with their relative contribution to soil exploration, strongly influences the capacity of the plant to acquire resources efficiently.

2.5 Root system development in maize

In maize (*Zea mays*) , root system development follows a chronological succession of distinct root types formed during different developmental stages (Hochholdinger & Zimmermann, 2008). The maize root system is composed of an embryonic root system, including the primary root (PR) and SRs and a post-embryonic root system composed of shoot-borne roots (Figure 2) (Hochholdinger et al., 2004).

The PR emerges first during germination and grows mainly vertically, contributing to early plant anchorage and water uptake (Perkins & Lynch, 2021). SRs then emerge from the base of the mesocotyl. These roots generally display shallow growth angles that favour exploration of the topsoil (Perkins & Lynch, 2021). SRs also have a smaller diameter than later axial roots, making them metabolically efficient during early seedling establishment, when seed reserves and photosynthate production remain limited (Perkins & Lynch, 2021).

As development progresses, the post-embryonic root system becomes dominant. Shoot-borne roots emerge successively from stem nodes located belowground, forming crown roots and later from aboveground nodes, forming brace roots (Feldman, 1994; Hochholdinger et al., 2004). Together, crown and brace roots are referred to as nodal roots. Maize plants typically develop up to six underground crown root nodes and several additional brace root nodes aboveground (Hochholdinger et al., 2004). These nodal roots constitute the major component of the mature maize root system and contribute substantially to water and nutrient acquisition during vegetative growth (Hochholdinger & Zimmermann, 2008). In field-grown maize, the majority of N uptake is associated with the development of these later nodal roots, beginning approximately four weeks after planting (DeBruin et al., 2017).

All major axial root classes, including primary, seminal and nodal roots, produce LRs of first and second order (Postma et al., 2014). The primary, seminal, crown and brace roots are collectively referred to as axial roots, whereas roots originating from these axes are termed LRs (Pagès & Pellerin, 1994). Differences in growth angle among these root classes contribute to soil exploration at different depths. SRs generally favour topsoil exploration through shallow growth angles, whereas nodal roots often display steeper growth angles that promote deeper soil exploration later in development (Dathe et al., 2016).

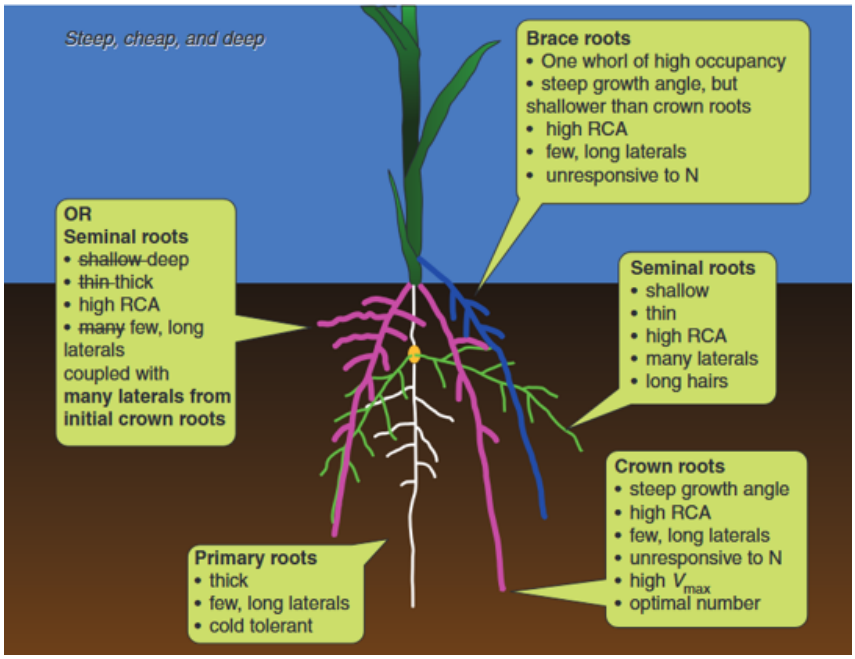

Figure 2: **Representation of the different root classes composing the maize root system**, including primary roots, seminal roots, crown roots and brace roots, together with their main architectural characteristics. The figure also illustrates the "steep, cheap and deep" ideotype proposed to improve N and water acquisition through optimized root architecture (J. P. Lynch, 2013).

2.6 RSA models

Studying root systems is particularly challenging because roots develop belowground and continuously interact with a highly heterogeneous environment (Dunbabin et al., 2003a). Root growth, nutrient availability, soil properties and water distribution all vary across space and time, generating complex interactions that are difficult to capture experimentally. Consequently, modelling approaches have become valuable tools for investigating RSA and understanding its relationship with resource acquisition (Dunbabin et al., 2003b).

Root models make it possible to investigate the functioning of different root architectures under a wide range of environmental conditions in a relatively short time. Modelling allows the comparison of root systems across different soil types, climatic conditions, management practices and nutrient distributions, which would be difficult to achieve experimentally (Dunbabin et al., 2003b). These approaches can therefore help identify promising root phenotypes and candidate traits for breeding programs aiming to improve crop productivity while reducing environmental impacts linked to nutrient losses (Dunbabin et al., 2003a).

Root modelling studies have also been instrumental in the development of root ideotypes, defined as combinations of architectural, anatomical and physiological traits expected to improve resource acquisition under specific environmental conditions. One of the best-known examples is the "Steep, Cheap and Deep" ideotype proposed by Lynch (J. P. Lynch, 2013) for maize. Based on the premise that water and nitrate tend to become increasingly available in deeper soil layers

over time, this ideotype promotes rapid exploration of deep soil horizons while minimizing the metabolic cost of root growth through a combination of architectural and anatomical traits. Such ideotypes provide useful conceptual frameworks for identifying root traits that may improve N and water acquisition and guide breeding strategies.

However, because of the complexity of root–soil interactions, models generally rely on simplifications. Processes such as the metabolic cost of root growth, nutrient transport, or changes in soil physical and chemical properties are often represented in simplified ways (Dunbabin et al., 2003a). Pagès et al. explained that modelling all soil physical and chemical dynamics at the root scale would be unnecessarily complex for short-term simulations because of the strong heterogeneity of soil properties. They therefore adopted a simpler stochastic approach in the RootTyp model (Pagès et al., 2004).

An important contribution of root modelling studies has been to demonstrate that nutrient availability should not be considered uniform throughout the soil profile, since nutrient supply varies spatially and temporally (Dunbabin et al., 2003a). Using a three-dimensional root growth model, Dunbabin et al. compared sparsely branched "herringbone" root systems with highly branched "dichotomous" architectures for nitrate acquisition in heterogeneous soils (Dunbabin et al., 2004). Their results showed that the efficiency of a root architecture depends strongly on the spatial and temporal distribution of nitrate in the soil. More broadly, root modelling studies have highlighted the importance of specific architectural traits, such as root branching patterns and growth angles, in determining the capacity of plants to acquire soil resources under different environmental conditions.

2.7 Root plasticity in heterogeneous environments

Root systems can respond to the heterogeneity of the soil through modifications of root growth and development according to local environmental conditions (Figure 3) (Awasthi & Laxmi, 2021). This plasticity is considered an essential feature for improving nutrient acquisition under limiting conditions (Gao et al., 2015).

Two major mechanisms of root plasticity are commonly described: enhanced root proliferation in nutrient-rich zones and elevate uptake kinetics (Dunbabin et al., 2004, 2003b; Robinson, 1994). Under low N conditions, root systems may respond locally by stimulating LR elongation in nitrate-rich patches, while systemic signalling pathways integrate the N status of the whole plant to regulate overall root development (Mishra et al., 2024). Root plasticity therefore results from the integration of both local soil signals and whole-plant nutrient status (Postma et al., 2014).

Local root proliferation can substantially improve nutrient acquisition in heterogeneous soils. Hodge et al. showed that root proliferation within an organic N-rich patch increased N capture in situations of interspecific competition (Hodge et al., 1999). Their study demonstrated that

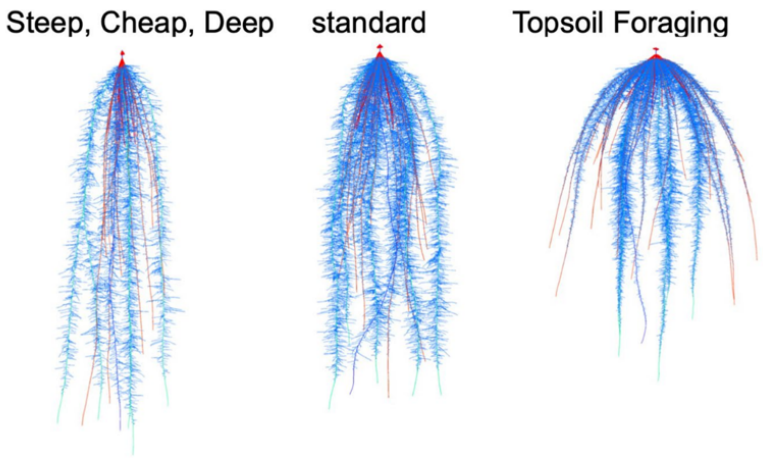

Figure 3: **Comparison of contrasting maize root system architectures generated through root system modelling**, illustrating different root foraging strategies: the "Steep, Cheap and Deep" ideotype characterized by deeper and steeper rooting, a standard root system architecture and a "Topsoil Foraging" architecture characterized by shallower root growth. These simulated architectures illustrate how root system organization can influence resource acquisition under different environmental conditions and nutrient distributions (J. P. Lynch et al., 2024).

the advantage mainly resulted from a greater density of roots in the nutrient-rich zone rather than from increased nutrient uptake activity per unit of root length. These results highlight that the efficiency of N acquisition depends strongly on the spatial distribution of nutrients and on competitive interactions within the soil environment and that root plasticity can provide a competitive advantage in heterogeneous soils (Hodge et al., 1999).

Plastic responses vary with plant species, nutrient type, plant demand, the spatial scale and temporal stability of nutrient heterogeneity, plant age and competition between plants (Dunbabin et al., 2003b). This complexity partly explains why the functional interpretation of root plasticity remains difficult (Postma et al., 2014).

2.8 Cost of the root system

Root systems are metabolically costly organs whose construction and maintenance require substantial investments of carbon, nutrients and energy (J. P. Lynch, 2015). Root growth and functioning involve several processes that contribute to these costs, including respiratory energy expenditure, biomass maintenance and the uptake and transport of mineral ions (Dunbabin et al., 2003a, 2003b). In addition, root growth competes with other plant functions for internal resources such as photosynthates, N and phosphorus, especially under edaphic stress conditions where plants allocate proportionally more resources to roots relative to shoots (J. P. Lynch, 2022).

The cost of root systems is difficult to quantify because it varies according to numerous factors, including plant age, root age and root type, environmental conditions, season, plant stress and

symbiotic interactions (Dunbabin et al., 2003a). Root system volume is often used as a proxy for root cost because carbon requirements for growth, maintenance and respiration generally increase with the amount of root tissue produced, particularly with the number of cortical cells (Dunbabin et al., 2003b).

Because of these metabolic constraints, larger root systems are not necessarily more efficient for nutrient acquisition. Producing and maintaining more roots than required for N capture may become counterproductive by diverting plant resources away from other important functions, including shoot growth or the exploration of new soil domains (J. P. Lynch et al., 2024). Root system efficiency therefore depends on a balance between resource acquisition and the metabolic costs associated with soil exploration.

2.9 Root traits associated with low N availability

Root phenotypes associated with improved N acquisition under low N conditions generally favour efficient soil exploration while limiting metabolic costs. However, because N availability varies according to agroecosystems, soil texture and leaching intensity, there is no universally optimal RSA (Dunbabin et al., 2003b). In low-input systems, N is often concentrated in the topsoil through mineralization of organic matter, whereas in fertilized systems nitrate progressively moves toward deeper soil layers through leaching (J. P. Lynch et al., 2024). Consequently, root phenotypes favourable for N acquisition depend strongly on the spatial and temporal distribution of N in the soil.

2.9.1 Biomass allocation and root elongation

Under low N conditions, plants generally allocate proportionally more resources to root growth relative to shoot growth. Increased R:S ratios are commonly associated with nutrient deficiencies and reflect greater carbon allocation toward the root system (Dathe et al., 2016). In maize, Gao et al. showed that low N treatment increased the R:S ratio, initially because of both increased root biomass and reduced shoot growth and later mainly because of reduced shoot development (Gao et al., 2015). N concentration also decreased more strongly in shoots than in roots, suggesting preferential allocation of limited N resources toward the root system in order to sustain root growth (Gao et al., 2015).

Low N is also known to stimulate root elongation (Gao et al., 2015). In maize, low N increased the length of primary, seminal and crown roots, suggesting that enhanced axial root elongation is an important acclimation response to N deficiency (Gao et al., 2015). This response may improve subsoil exploration and nitrate capture, especially because nitrate leaching often occurs early in the season before the root system is fully developed (J. P. Lynch, 2022). Enhanced elongation under low N has been associated with increased mature cell length and modifications

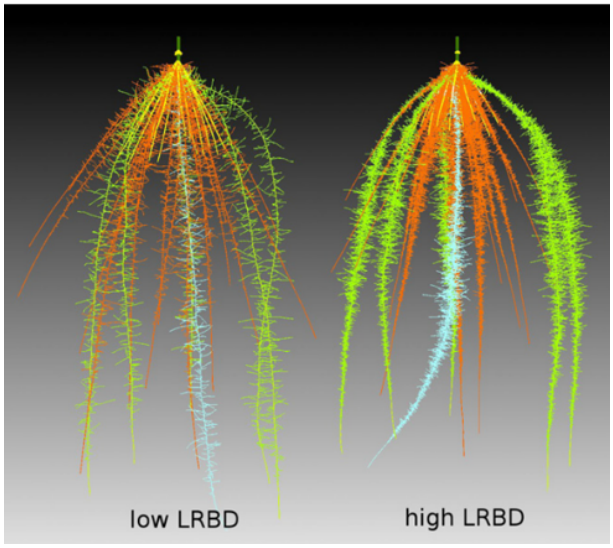

Figure 4: **Illustration of maize root system architectures generated by a root architecture model, showing contrasting lateral root branching densities (LRBD)**: a sparsely branched genotype (left) and a highly branched genotype (right). Differences in lateral root density modify the spatial organization of the root system and may influence soil exploration, metabolic costs and nutrient acquisition (Postma et al., 2014).

of radial root anatomy, including reduced root thickness, which may lower the metabolic cost of elongation under nutrient limitation (Gao et al., 2015).

2.9.2 Lateral root branching density

Lateral root branching density (LRBD) strongly influences the balance between soil exploration efficiency and metabolic cost. Considerable genetic variation in LRBD exists in maize, ranging from very sparse to highly branched root systems (Figure 4) (Postma et al., 2014). Increased branching can enhance total root length and nutrient acquisition, but also increases root competition and metabolic costs associated with root construction and maintenance (Postma et al., 2014).

The optimal LRBD differs depending on the nutrient considered. High branching densities are generally advantageous for phosphorus acquisition. In contrast, lower LRBD is generally more favourable for nitrate acquisition (Postma et al., 2014; Rangarajan et al., 2022). Postma et al. showed that maize phenotypes with fewer but longer LRs developed deeper root systems and improved N capture under low N availability (Postma et al., 2014). These “few/long” phenotypes also improved shoot N status, photosynthesis, growth and yield under low N conditions in both greenhouse and field experiments (Zhan & Lynch, 2015).

Reduced LRBD may also conserve N and carbon resources for axial root elongation. Gao et al. suggested that fewer and shorter LRs under prolonged low N conditions may contribute to sustaining axial root growth and deeper soil exploration (Gao et al., 2015). Nevertheless, some degree of fine LR development remains important because higher-order laterals contribute

substantially to root length density and nitrate uptake efficiency while requiring relatively low additional root volume (Dunbabin et al., 2003b).

2.9.3 Axial root growth angle

Axial root growth angle is one of the major determinants of rooting depth and therefore strongly influences N acquisition (Dathe et al., 2016; Trachsel et al., 2013). Shallow root systems are generally more efficient for acquiring immobile nutrients whereas steeper root systems favour the capture of mobile resources (Schneider et al., 2022).

Substantial genetic variation for root growth angle exists in maize germplasm (Hochholdinger et al., 2004). Several studies have shown that steeper crown root angles are associated with deeper rooting and improved N capture (Schneider et al., 2022; Trachsel et al., 2013). Dathe et al. demonstrated that root growth angle affects N capture by modifying the spatial coincidence between root exploration and nitrate availability (Dathe et al., 2016). Under conditions of important nitrate leaching, steeper root systems improve access to deep nitrate pools. However, extremely steep root systems may become counterproductive because roots tend to converge within a narrow soil volume, leading to overlap in resource foraging and increased competition among roots of the same plant (Dathe et al., 2016; Rangarajan et al., 2022).

Overall, steeper axial root angles are considered promising targets for breeding programs aiming to improve N and water acquisition under edaphic stress conditions (J. P. Lynch, 2022; Schneider et al., 2022).

2.9.4 Axial root number

The number of axial roots is another important architectural trait influencing N acquisition. Producing many axial roots increases the metabolic cost of the root system and intensifies competition among roots of the same plant for both soil N and internal resources such as carbohydrates (J. P. Lynch et al., 2024). Conversely, too few axial roots may limit soil exploration and increase sensitivity to root loss. An optimal number of axial roots is therefore expected for efficient N capture (J. P. Lynch, 2013).

Several studies suggest that maize phenotypes with fewer axial roots can allocate more resources to the elongation of existing roots, resulting in deeper rooting and improved capture of deep soil nitrate (J. P. Lynch, 2013). Reduced numbers of crown roots are one component of the “Steep, Cheap and Deep” ideotype proposed for efficient acquisition of N and water (J. P. Lynch, 2013). Under low N conditions, maize plants often reduce the production of later-emerging crown roots, possibly because limited N availability cannot support the development of all root axes (Gao et al., 2015).

In contrast, seminal roots (SRs) appear particularly important during early seedling establishment. Perkins and Lynch estimated that SRs account for about one-third of N capture during the first 25 days of maize growth (Perkins & Lynch, 2021). Increasing SR number may therefore improve early N acquisition, provided that seed carbohydrate reserves can support the additional root investment (Perkins & Lynch, 2021). Multi-objective optimization studies further suggest that optimal N-acquisition phenotypes combine relatively low axial root numbers with low LRBD and contrasting root angles that maximize soil exploration while minimizing carbon costs (Rangarajan et al., 2022).

2.10 Maize landraces

Modern agriculture mainly relies on hybrid varieties selected for their high and stable yields across a wide range of environments. However, modern agriculture relies on a relatively limited number of commercially successful genotypes, resulting in lower genetic diversity within cultivated fields compared with traditional populations such as landraces (Azeez et al., 2018; Hölker et al., 2019). Although modern hybrids generally provide high productivity under favorable conditions, this reduced diversity may limit their adaptability to environmental stresses and changing climatic conditions.

In contrast, landraces are locally cultivated populations that have been maintained by farmers over long periods of time and are characterized by high levels of genetic diversity and heterogeneity (Villa et al., 2005). Their evolution results from the combined effects of natural selection, farmer selection and local environmental conditions, leading to populations specifically adapted to their region of cultivation (Casañas et al., 2017). Unlike genetically uniform modern varieties, landraces constitute reservoirs of genetic variation that are shaped by local environmental conditions and farmer selection practices over time (Casañas et al., 2017).

Because of their local adaptation, maize landraces could play an important role in the development of low-input agricultural systems. They may represent valuable sources of alleles that are absent, rare or underutilized in current breeding programs (Azeez et al., 2018). These traditional populations often possess traits associated with adaptation to limiting environmental conditions, including tolerance to abiotic and biotic stresses (Azeez et al., 2018; Prasanna & Sharma, 2005). Therefore, landraces represent a valuable complementary resource for breeding programs seeking to enhance crop resilience and diversify the genetic resources available for crop improvement. In addition, their long-term adaptation to specific local environments makes them particularly relevant for the development of agricultural systems adapted to local environmental and management conditions.

3 Objectives

The main objective of this master's thesis was to investigate how root system architecture responds to contrasting N conditions in a panel of *Zea mays* varieties.

The research questions addressed in this study were:

- How do maize varieties differ in their phenotypic responses to contrasting N conditions?
- Do varieties with contrasting N use efficiency (High NUE and Low NUE) exhibit different root architectural responses under low N conditions?

The main hypotheses of this study were that:

- maize plants grown under low N conditions allocate proportionally more resources to root development than to shoot growth;
- varieties with high N use efficiency (High NUE) display enhanced growth and root development under low N conditions compared to low NUE varieties;
- the different maize varieties exhibit contrasting phenotypic and architectural responses to N availability;
- hybrid varieties exhibit distinct growth and root architectural responses compared with landraces.

A first experiment was conducted on a single maize variety to identify the most suitable N conditions for the experiment performed on the RootPhAir platform. This experiment also aimed to evaluate different seedling anchorage solutions. The N conditions tested were 0.5N, 1N, 1.5N, 3N and 6N. Based on the observed responses, the concentrations selected for the subsequent experiment was 0.5N and 3N, representing contrasting N conditions.

A second experiment was then conducted on the RootPhAir platform with two independent replicates to evaluate the effects of contrasting N concentrations on phenotypic traits and RSA among maize varieties. The two replicates followed the same experimental design and objectives, with the exception that N treatments were inverted between tanks in the second replicate to assess potential tank-position effects on plant responses.

4 Materials and Methods

Experiments were conducted in the Plant Ecology, ecoPhysiology and sustainable Agriculture (PEPA) lab, from the Earth and Life Institute Agronomy, from the UCLouvain, in Belgium. Two experiments were carried out in the SeFy greenhouse,. The first one, in November 2025, was a preliminary experiment made in small aeroponic tanks. The second one was performed in root phenotyping platform of UCLouvain (RootPhAir, part of EMPHASIS ESFRI) and comprised two full replicates, in December 2025 and March 2026.

4.1 Plant Materials and Growth Conditions

For the first experiment, the organic maize variety BELAMI was used. For the second, 13 varieties were used: eight European maize landraces and five hybrid varieties. Among the landraces, four were classified as high nitrogen-use efficiency (High NUE) and four as low nitrogen-use efficiency (Low NUE) (Table 1). These classifications were based on field results obtained by collaborators within the framework of the MineLandDiv project.

Table 1: Varieties used in the second experiment in the RootPhAir platform, including type, NUE classification, origin and study code.

Name	Type	Classification	Origin	Study code
ITA0370114	Landrace	High NUE	Italy	MLD_043
ITA0370152	Landrace	Low NUE	Italy	MLD_050
ESP009-ZMV0505	Landrace	High NUE	Spain	MLD_099
PI527477	Landrace	Low NUE	Algeria	MLD_156
FRA0411546	Landrace	High NUE	Spain	MLD_176
FRA0410194	Landrace	High NUE	France	MLD_215
FRA0410641	Landrace	Low NUE	France	MLD_226
SVGB-7774	Landrace	Low NUE	Romania	MLD_306
B73 x PH207	Hybrid	Hybrid	–	MLD_C002
KWS Kamparis	Hybrid	Hybrid	–	MLD_C004
KWS Kerubino	Hybrid	Hybrid	–	MLD_C005
ES Faraday	Hybrid	Hybrid	–	MLD_C006
Cardif	Hybrid	Hybrid	–	MLD_C007

Seeds were washed for 5 minutes in a 20% bleach solution, then rinsed five times for 5 minutes each with deionized water (see Appendix A). Subsequently, they were placed to germinate on filter paper in a dark chamber at 28 °C for 48 hours.

After germination, the seeds were transferred to the platform and placed in plugs. Backup seeds were also germinated to replace seeds whose primary root was damaged during transfer were

replaced the following day. The plugs were watered during transfer to ensure that seedlings develop in an hydrated environment. For the first three days, the seedlings were supplied with deionized water. On the third day, the nutrient solutions were applied and subsequently renewed on a weekly basis.

In the greenhouse, a 16 h light / 8 h dark photoperiod was maintained at a set temperature of 22 °C. Illumination was provided by eight VEGELED Pandora LB680 horticultural LED floodlights, with four lamps positioned above each tank. The lighting system was adjusted to provide a photosynthetic photon flux density (PPFD) of approximately 180 μmol m^{-2} s^{-1}. Each replicate was conducted over a three-week period. Temperature and relative humidity were continuously monitored during the experiment and the corresponding data are presented in Appendix B.

The **preliminary aeroponic setup** (Figure 5) consisted of a 40x60 cm PVC solution container and a 60-cm tall vertical polystyrene structure supporting 35 extruded horizontal polystyrene strips in which three or four 22 mm holes were drilled to insert various seed holders. Each platform accommodated up to 125 plants.

Each system was equipped with a Shui Zhi Yuan (caravan) pump and a filter. The nutrient solution was sprayed through plastic nozzles (Gardena) onto the roots through a circuit connected to the pump.

No imaging was performed, as the objective of the experiment was limited to selecting appropriate N concentrations and plug types based solely on measurements made at harvest.

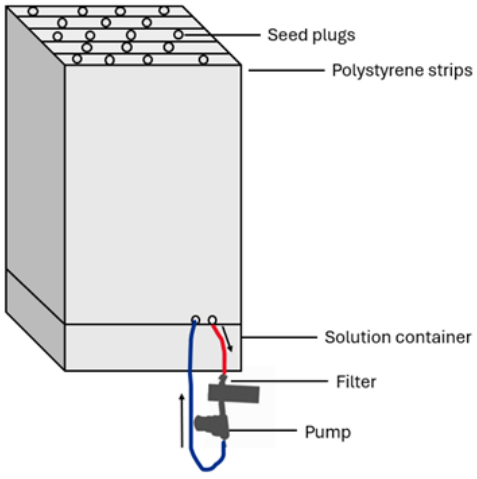

Figure 5: Simplified schematic of the aeroponic growth system showing the seed plugs placed in perforated polystyrene strips above the nutrient solution container. The solution is recirculated through a pump and filter system.

As depicted in Figure 6, the **RootPhAir platform** consists of two aeroponic tanks, each accommodating 495 plants and located within the same greenhouse. In each tank, plants were arranged on strips of five, with a total of 99 strips per tank. Nutrient solution was delivered directly to the roots by stainless steel sprinklers positioned at the bottom of the tanks.

Within this setup, the strips moved continuously, enabling high-throughput phenotyping of up to 990 plants per replicate. Under standard operating conditions, each plant was imaged every two hours. To facilitate individual tracking, each plant was equipped with an RFID tag, allowing the system to automatically identify plants and sort the corresponding images.

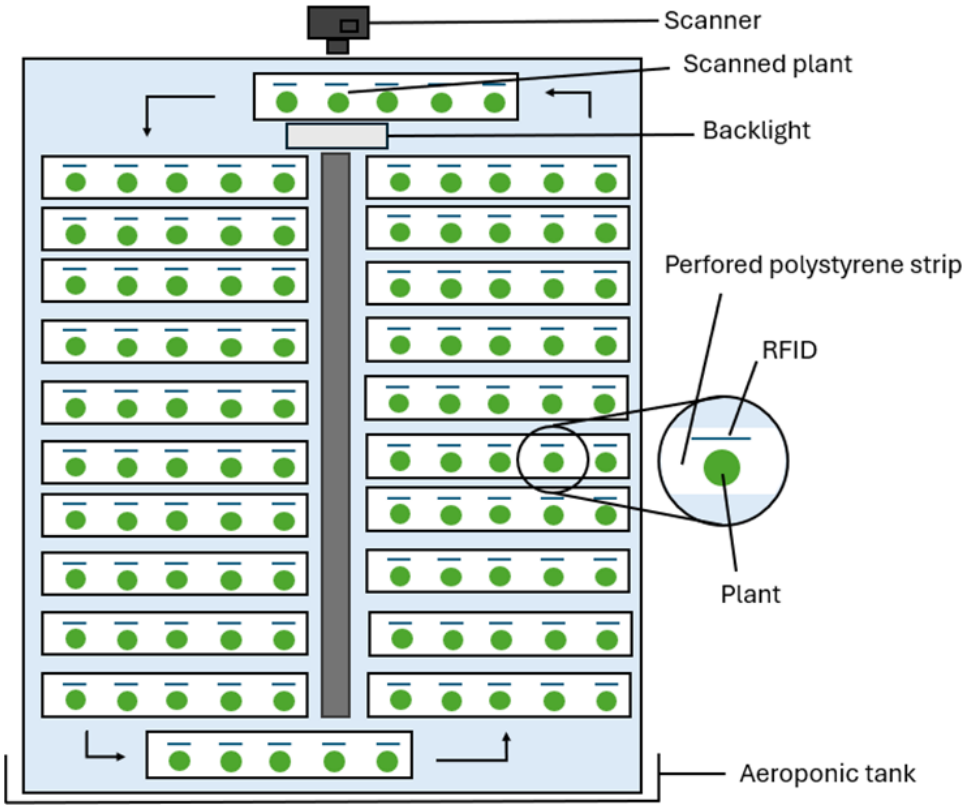

Figure 6: Simplified top-view diagram of one of the RootPhAir platform trays. The movements of the polystyrene strips are indicated by the black arrows.

The **nutrient solutions** were based on a modified Hoagland solution, in which N concentrations were adjusted depending on the treatment (see Appendix D). N was supplied in both nitrate (NO_3^-) and ammonium (NH_4^+) forms using KNO_3, $Ca(NO_3)_2$ and NH_4NO_3.

The relative proportions of these sources were maintained while varying the total N concentration. To allow independent adjustment of N levels without affecting potassium supply, potassium was provided separately using K_2SO_4. Calcium was supplemented using $CaSO_4 \cdot 2H_2O$ (gypsum) to compensate for reduced inputs from calcium nitrate. The nutrient solution contained the following macro- and micronutrients: K_2SO_4, $Ca(NO_3)_2 \cdot 4H_2O$, $MgSO_4 \cdot 7H_2O$, NH_4NO_3, $CaSO_4 \cdot 2H_2O$, KH_2PO_4 and trace elements including H_3BO_3, $MnCl_2 \cdot 4H_2O$, $ZnSO_4 \cdot 7H_2O$, $CuSO_4 \cdot 5H_2O$, H_2MoO_4 and Fe-EDTA ($C_{10}H_{12}N_2FeNaO_8$).

Nutrient solutions were prepared in 25 L containers. The container were pre-filled with 15 L of deionized water, followed by the reagents and the final volume was adjusted to 25 L. The pH was corrected to 5.0 using 3 M KOH.

The RootPhAir platform operates as a closed-loop system in which the nutrient solution is continuously recirculated. Consequently, the electrical conductivity (EC) of the solution may

change over time due to water uptake and nutrient absorption by the plants. In the second replicate, EC was measured when the nutrient solutions were first applied, then monitored each morning and adjusted as needed by adding either water or nutrient solution to maintain values close to the target value. The same procedure was followed for pH, with daily measurements and adjustments using 3 M KOH.

4.2 Experimental Design

Five N concentrations were tested in the preliminary experiment (0.5N, 1N, 1.5N, 3N and 6N), each being assigned to a different aeroponic box. Each box contained 25 plants distributed across seven strips holding three or four plants each, resulting in a total of 125 plants for the experiment.

In addition to the standard plugs used to support seedlings within the RootPhAir platform, two alternative anchorage systems were evaluated (Figure 7). These alternatives consisted of bioplastic baskets of two different sizes (small and medium) filled with perlite and vermiculite, which were tested as potential substitutes for the standard plugs (seedling support devices see Appendix B). In boxes A, C and E, strip 4 contained three medium baskets and strip 5 contained four small baskets. In boxess B and D, strip 4 contained three small baskets and strip 5 contained four medium baskets. All remaining holes were equipped with standard plugs.

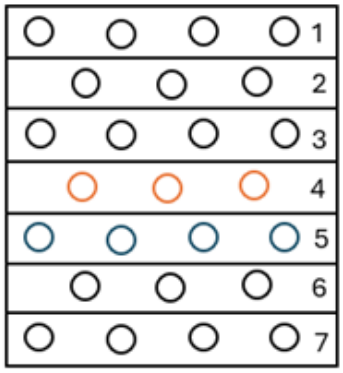

Figure 7: Design for the first experiment. In A,C and E , orange correspond at medium plugs and blue at small plugs. In B and D , orange correspond at small plugs and blue at medium plugs.

In the second experiment, two N concentrations were tested (0.5N and 3N). In the December replicate, the 0.5N treatment was assigned to tank A and the 3N treatment to tank B. The opposite was made in the March replicate. The experimental design was generated in RStudio using the `DiGGer` package (Coombes, 2020). using four independent row-column design (one per tank and replicate).

Since each strip contained five plants, blocks of three strips were defined. These blocks were complete for the genotype factor (8 landraces + 5 hybrids) and were nested in the tank factor. With 99 strips per tank, this resulted in 33 blocks per tank. The design was constrained to ensure

that each variety appeared a similar number of times within each column. Consequently, in each column, six varieties were represented six times and nine varieties were represented seven times, although these were not the same varieties across columns.

Overall, the design provided 33 plants per variety within each N treatment (i.e., per tank) and replicate, resulting in a total of 132 plants per variety across the whole experiment.

4.3 In Situ Measurements

In RootPhAir, images were automatically captured. Under optimal conditions, each plant was imaged every two hours. For the experiment conducted during this master's thesis, there were 20 to 25 pictures for first replicate and 40 to 45 pictures for the second replicate.

From day 11 onward, when the first ligulation of the second leaf were observed in the experiment , all plants were monitored daily to determine the precise day of ligulation for each individual plant. On that day, a SPAD measurement was performed on the second leaf, with the greenhouse light turned off during the measurement.

Three readings were taken around the middle of the leaf, on both sides of the midrib and their average was calculated. This procedure was repeated daily for all plants reaching ligulation on that particular day until all plants had been measured.

4.4 Harvest

Harvest was carried out in two batches, based on the developmental stage of the second leaf (ligule emergence). Plants in which the ligule emerged earlier on the second leaf were harvested first. At harvest, a new SPAD measurement was taken on the second leaf. The number of ligulated leaves was also recorded. Roots and shoots were then separated and the fresh weight of each part was measured. Subsequently, the samples were placed in an oven for at least 48 hours at 60 °C, after which dry weight of roots and shoots was recorded.

4.5 Derived variables

Several variables were derived from the measurements collected during the experiment.

The **root-to-shoot ratio** was obtained by dividing root dry biomass by shoot dry biomass.

SPAD variation on the second leaf was calculated differently depending on the experiment. For Experiment 1, it corresponded to the difference between the SPAD value measured on day 13 and the value measured at harvest (day 20). For the second experiment , SPAD variation

was calculated as the difference between the SPAD value measured at ligule emergence on the second leaf (D0) and the value measured at harvest.

2nd leaf age was defined as the time elapsed, expressed in days, between ligule emergence on the second leaf and harvest.

Shoot and root water contents were calculated according to the following formula:

$$\text{Water content} = \frac{FW - DW}{FW}$$

where FW corresponds to fresh weight and DW to dry weight.

Finally, a **state** column was created to identify plants presenting anomalies. Dead plants, unusually small plants observed either during harvest or image analysis and plants whose development had been visibly affected by experimental incidents were recorded in this column.

4.6 Image analysis

RSA traits were extracted from images using two complementary image-analysis workflows. Static architectural traits, including seminal root (SR) and lateral root (LR) angles, were measured using the program Aeroscan based on the ImageJ Java library. Dynamic developmental traits were extracted from time-series images using the Python software *Aerogrow*. Both programs were developed in house for root architecture/growth analysis on the RootPhair platform.

4.6.1 Aeroscan

SR and LR angles were measured from images acquired during the experiment. SR angles were measured before the emergence of LRs to ensure that all SRs were fully visible and could be distinguished without interference from branching. At the same developmental stage, the number of SRs was also recorded.

LR angles were measured on three different images whenever possible. To better capture within-plant variability, measurements were preferentially performed on different roots and, when available, at different observation times.

A confidence score was assigned to each measurement in order to identify roots presenting anomalies or image-quality issues that could affect measurement accuracy. These confidence score are described in Appendix F and were subsequently used during data cleaning.

4.6.2 Time series images analysis: Aerogrow

Dynamic root traits were extracted from time-series images using *Aerogrow*. The software combines root tracking and temporal information from successive images to quantify root growth and developmental processes. The traits measured included SR elongation rate, LR elongation rate, LR density and duration of primordium development (DPD).

SR elongation rate was estimated from the displacement of the longest root tip over time. For each image, the geodesic distance between the seed and the root tip was determined along the root trajectory. Elongation rate was then calculated as the slope of the relationship between root length and plant age and expressed in cm day^{-1}.

The duration of primordium development (DPD) was defined as the time interval between the passage of a SR through a given position and the emergence of a LR at that same position. The position of each emerged LR was projected onto the SR growth trajectory. The age of the SR when it crossed this position was estimated from its elongation dynamics and compared with the age at which the LR became visible. DPD was expressed in hours and represents the time elapsed between LR initiation and emergence.

LR density was measured within a predefined region of interest where both newly emerged and rapidly growing LRs were clearly visible. Density was calculated as the number of emerged LRs divided by the length of SR included within the region of interest and was expressed as the number of LRs per centimeter of SR.

LR elongation rate was estimated in the same region by relating the length of individual LRs to their age, calculated as the time elapsed since their emergence (Figure 8). For each plant, a linear regression was fitted between LR length and LR age and the slope of this relationship was used as an estimate of mean LR elongation rate (cm day^{-1}).

Specific confidence codes were assigned throughout the analysis to identify roots presenting anomalies or measurement issues (Appendix G). These annotations were subsequently used during data cleaning to exclude unreliable measurements from the statistical analyses.

4.7 Statistical analyses

Non-germinated seeds and plants that were substantially smaller than others within the same treatment were removed from the dataset. These observations were identified either during the experiment or at harvest.

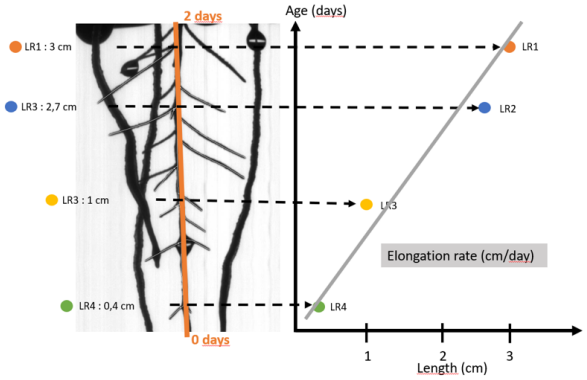

Figure 8: Schematic representation of lateral root elongation rate estimation. The age of each lateral root was calculated as the time elapsed since its emergence. For a given plant, lateral root length was plotted against lateral root age and a linear regression was fitted. The slope of the regression corresponds to the mean lateral root elongation rate (cm day^{-1}).(Lengrand, 2026)

4.7.1 Data preprocessing

For each trait, potential outliers were identified using a z-score threshold of 3. Z-scores were calculated from the residual of trait values predicted by a simplified linear model (Equation 4.1). Observations exceeding this threshold were inspected and removed when justified.

$$Y = G + N + G : N + G : V + G : V : N \tag{4.1}$$

All categorical variables describing the experimental design (N treatment, variety, experimental tank, row block and column block) were defined as factors. 2nd leaf age was treated as a continuous variable and centered around its mean value prior to analysis.

4.7.2 Linear mixed models and estimation of adjusted means

Trait responses were analysed using linear mixed-effects models fitted using the `lme4` package in R (Bates et al., 2015). For each trait, the fixed-effects structure included nitrogen treatment (*N*), variety group (*G*; high-efficiency landraces, low-efficiency landraces and hybrids), variety nested within group (*G:V*) and their interactions (*G:N* and *G:V:N*) when supported by the data. The replicate–tank combination (*R_T*), corresponding to each replicate × tank combination, was included as a fixed effect to account for differences between experimental runs and tanks.

To account for the spatial organisation of plants within the RootPhAir platform, row block and column block nested within replicate–tank combination were included as random effects. 2nd leaf age (*AGE_c*), defined as the centered number of days between ligule emergence and harvest, was included when relevant to account for developmental differences among plants.

Several candidate model structures differing in their fixed and random effects were evaluated for each trait. The final model retained for each trait was selected based on Akaike's Information

Criterion (AIC), the significance of model terms and biological relevance, particularly regarding the inclusion of 2nd leaf age. The different candidate models tested during the model selection procedure are presented in Appendix H. Model assumptions were assessed through visual inspection of residual distributions and residual-versus-fitted value plots.

The final models can be generally represented as:

$$Y = G + N + G:N + G:V + G:V:N + R_T + (1|Row) + (1|Col) + (1|AGE_c) \quad (4.2)$$

where G represents variety group, N nitrogen treatment, V genotype nested within group and R_T the replicate–tank combination. *Row* and *Col* correspond to the row and column blocks nested within replicate–tank combinations, while *AGE_c* represents the centered age of the 2nd leaf.

Estimated marginal means (EMMs) were calculated from the final fitted models using the `emmeans` package (Lenth, 2025). EMMs were obtained for each genotype within each N treatment (`~V | N`) and were used to estimate adjusted trait values while accounting for the effects retained in the final model. These adjusted means were subsequently used to compare genotype responses across N treatments and to quantify phenotypic plasticity independently of environmental and spatial sources of variation.

4.7.3 Phenotypic plasticity

Phenotypic plasticity was calculated from the model-estimated means for each variety and trait. Relative plasticity was expressed as:

$$\frac{LowN - HighN}{HighN} \quad (4.3)$$

where *LowN* and *HighN* correspond to the estimated trait values under severe (0.5 N) and moderate (3 N) N limitation, respectively. Negative values indicate a reduction of the trait under severe N limitation, whereas positive values indicate an increase.

4.7.4 Multivariate analyses

Principal component analyses (PCA) were performed using the `FactoMineR` package on both adjusted trait values and plasticity indices (Lê et al., 2008). Prior to analysis, variables were centered and scaled to unit variance.

Relationships among traits were explored using Pearson correlation coefficients. Correlation matrices were visualized using the `corrplot` and `GGally` packages (Schloerke et al., 2025;

Wei & Simko, 2024). Only significant correlations ($p < 0.05$) were retained for graphical representation.

5 Results

5.1 Preliminary Experiment : selection of contrasting nitrogen conditions for root architecture analyses

Several N concentrations were tested in order to evaluate their effects on plant growth and physiology (Figure 9). Among the measured variables, root dry biomass and the root-to-shoot ratio were selected as the most relevant parameters to support the choice of N treatments, as they directly reflect root development and biomass allocation responses to N availability.

Figure 9: **Plants grown under different nitrogen treatments at day 20 of the preliminary experiment**, immediately before harvest. Visible differences in shoot development were observed among nitrogen conditions. From left to right: 0.5N, 1N, 1.5N, 3N and 6N.

The **root dry biomass** (Figure 10a) increased progressively with increasing N treatments. Higher N availability generally resulted in greater root biomass, although the mean biomass observed under the 6N treatment was slightly lower than under the 3N treatment. Lower variability was also observed for the 0.5N and 1N treatments.

ANOVA revealed a significant effect of N treatment on root dry biomass ($p < 0.001$). Pairwise comparisons using Tukey's HSD test showed that the 3N and 6N treatments had significantly higher root biomass than the 0.5N, 1N and 1.5N treatments. No significant difference was detected between the 3N and 6N treatments.

The **root-to-shoot ratio** (Figure 10b) decreased progressively with increasing N availability,

suggesting a greater allocation of biomass to aerial tissues under high N conditions.

ANOVA revealed a significant effect of N treatment on the root-to-shoot ratio ($p < 0.001$). Tukey's HSD test showed that all treatments (1N, 1.5N, 3N and 6N) had significantly lower ratios than the 0.5N treatment. In addition, the 3N and 6N treatments were significantly lower than the 1N and 1.5N treatments. No significant differences were observed between the 1N and 1.5N treatments, nor between the 3N and 6N treatments.

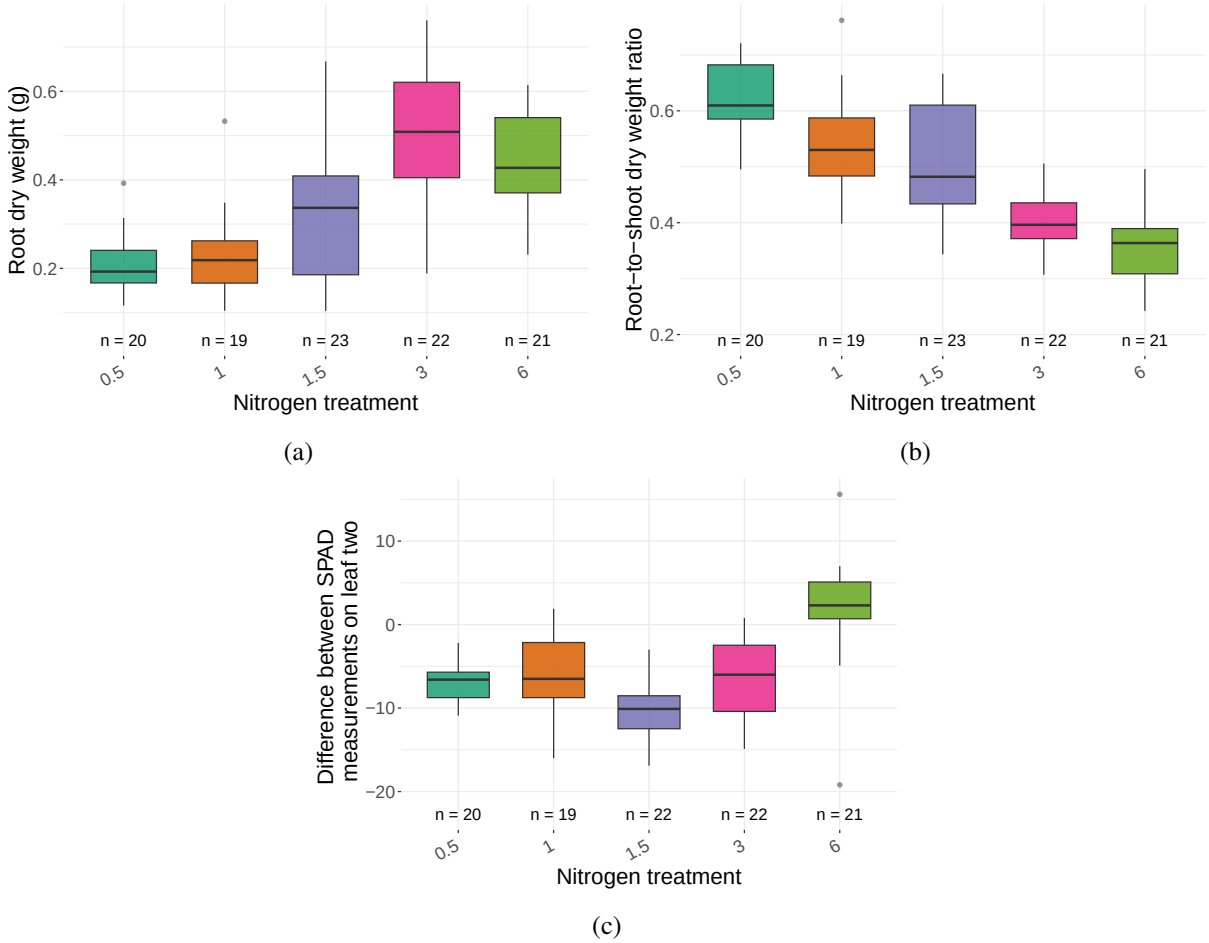

Figure 10: **Effect of nitrogen treatments on selected traits** after three weeks of growth during the preliminary experiment. (A) Root dry biomass, (B) root-to-shoot dry biomass ratio and (C) variation in SPAD values between the two measurement dates. Only plants without abnormalities recorded in the *state* column were included in the analysis. The number of observations (n) is indicated below each boxplot.

The **variation in SPAD values between the two measurement dates** (Figure 10c) showed a less pronounced trend than the other measured variables. However, the 6N treatment displayed noticeably higher values compared with the other N treatments.

ANOVA revealed a significant effect of N treatment on the variation in SPAD value ($p < 0.001$). Tukey's HSD test confirmed that the 6N treatment differed significantly from all other treatments, whereas no significant differences were observed among the 0.5N, 1N, 1.5N and 3N treatments.

For **SPAD measurements at day 13 and day 20** (Figure 11), only limited differences were

observed among N treatments. At day 13, the 6N treatment showed lower SPAD values compared with the other treatments. At day 20, SPAD values for the 1N treatment appeared slightly higher than for the other treatments, although a significant difference was only detected between the 1N and 1.5N treatments.

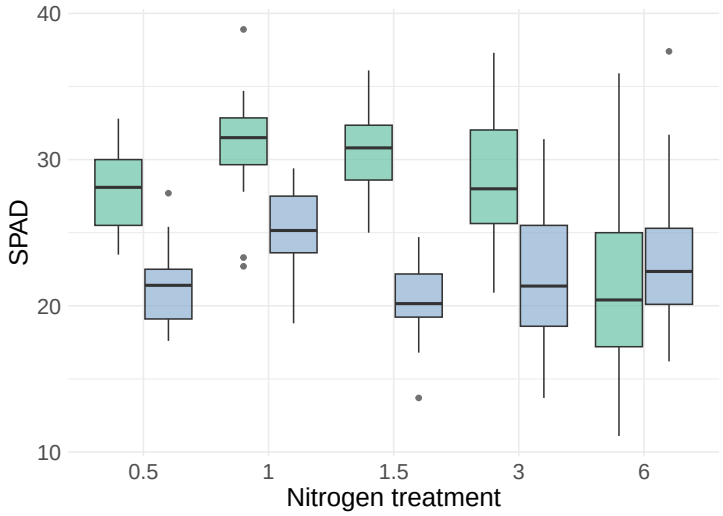

Figure 11: **Effect of N treatments on SPAD values** measured 13 days (green boxplots) and 20 days (blue boxplots) after the start of the experiment. Only plants without anomalies recorded in the state column were included in the analysis.

Discussion and justification of the selected nitrogen treatments

The increase in root biomass with increasing N availability suggests that higher nutrient supply promoted overall root growth and plant development.

The root-to-shoot ratio decreased with increasing N availability, indicating a progressive shift in biomass allocation toward aerial tissues. Under N limitation, plants typically allocate proportionally more biomass to roots presumably to increase nutrient foraging capacity and improve N uptake from the environment (Hermans et al., 2006).

The lower SPAD values observed at day 13 under the highest N treatment may be related to the chlorotic leaf symptoms (Figure 8) observed under these conditions, which could have affected SPAD measurements. Another possible explanation is the nitrogen dilution effect commonly observed during rapid plant growth. Under high N availability, plants may accumulate biomass more rapidly, leading to a decrease in nitrogen concentration within leaf tissues despite a greater overall nitrogen uptake. This process could explain why lower SPAD values were already observed at 6N at day 13. Additional analyses would be required to confirm these hypotheses.

Figure 12: **Leaf symptoms** observed under the highest N treatment (6N) at the end of the experiment. Plants grown under this condition showed marked longitudinal chlorosis patterns on the leaves.

The N conditions selected for the RootPhair experiments were 3N and 0.5N. The 3N concentration was chosen because it showed significant differences compared with the other tested concentrations and because it had already been used in previous MineLandDiv experiments. The second selected concentration was 0.5N. This treatment was selected because it showed significant differences compared with higher N concentrations while plants still remained in good condition after three weeks of growth. In addition, the root-to-shoot ratio clearly indicated that plants were responding to N limitation under this treatment.

Overall, this preliminary experiment successfully identified two contrasting N conditions suitable for further experiments on root architecture. These treatments induced significant differences in biomass allocation and physiological responses while maintaining plant viability throughout the experiment.

5.2 RootPhair experiment

During the second replicate, a technical failure caused the irrigation pump to stop operating for approximately eight consecutive hours during the night, resulting in a transient water deficit. Plants that exhibited severe symptoms following this event were excluded from the analyses. Significant differences among replicates were detected for all measured variables. However, because the overall patterns of response were consistent across replicates, all remaining data were retained for subsequent analyses. The only exception concerned SR elongation rate, for which the response pattern differed from that observed in the other replicate (Appendix F).

5.2.1 Trait responses to nitrogen limitation

Table 2 provides a synthetic overview of the linear mixed models fitted for each phenotypic trait. It revealed that N treatment was a major source of variation for most traits. Genotype group and genotype nested within group were also significant for the majority of traits, indicating

substantial genetic variation among varieties. In contrast, interactions involving N treatment were less consistently significant and depended on the trait considered.

Replicate-tank combination (R_T) had a significant effect on nearly all traits, highlighting the importance of environmental variation between experimental runs and tanks. The random effects associated with row and column blocks were generally retained and often significant, confirming the presence of spatial heterogeneity within the RootPhAir platform.

2nd leaf age (AGE_c) contributed significantly to variation in several biomass and physiological traits, including root dry weight, shoot dry weight, root water content, shoot water content, SPAD at ligule emergence and the difference between SPAD measurements. In contrast, most root architectural traits, such as root angles and SR number, were largely independent of 2nd leaf age. Overall, biomass and physiological traits appeared to be more strongly influenced by developmental stage, whereas root architectural traits were primarily driven by genotype and N availability.

Table 2: **Summary of the statistical models retained for each phenotypic trait**. Black cells indicate effects retained in the final linear mixed model. The significance of each effect is reported using the following notation: *** ($p < 0.001$), ** ($p < 0.01$), * ($p < 0.05$), NS ($p \geq 0.05$) and NA (effect not estimated). A slash (/) indicates that the corresponding effect was not included in the final model. *Abbreviations:* G = genotype group; N = nitrogen treatment; G:N = genotype group × nitrogen treatment; G:V = genotype nested within group; G:V:N = genotype nested within group × nitrogen treatment; R_T = replicate-tank combination; Row = row block nested within replicate-tank; Col = column block nested within replicate-tank; Age = centred 2nd leaf age (AGE_c).

	Fixed						Random			p_value								
	G	N	G:N	G:V	G:V:N	R_T	Row	Col	Age	G	N	G:N	G:V	G:V:N	R_T	Row	Col	Age
Dry weight of roots (g)	■	■	■	■	■	■	■	■	■	***	**	NS	***	***	***	***	***	***
Water content of roots	■	■	■	■	■	■	■	■		***	*	*	***	***	***	***	***	/
Dry weight of shoots (g)	■	■	■	■	■	■	■	■	■	***	***	NS	***	***	***	***	***	***
Water content of shoots	■	■	■	■	■	■	■	■	■	***	NS	NS	***	***	***	***	***	**
Dry weight root to shoot ratio	■	■	■	■	■	■	■	■		***	***	***	***	***	NS	***	***	/
SPAD at ligule emergence	■	■	■	■	■	■			■	***	***	***	***	***	***	/	/	***
Difference between SPAD measurements on leaf two	■	■	■	■	■	■	■	■	■	***	***	***	***	**	***	***	***	***
Seminal root width angle (deg)	■	■	■	■	■	■				***	NA	NS	***	NS	***	/	/	/
Lateral root width angle (deg)	■	■	■	■	■	■	■			**	***	NS	***	***	***	***	/	/
Number of seminal roots before branching	■	■	■	■	■	■	■			***	***	NS	***	NS	**	*	/	/
Elongation rate of seminal roots (cm/day)	■	■	■	■	■	■	■	■		***	***	NS	***	***	***	NS	*	/
Lateral root density (count/cm)	■	■	■	■	■	■	■	■		***	***	*	***	*	*	NS	*	/
Duration of primordium development (h)	■	■	■	■	■	■	■			NS	*	NS	**	NS	***	*	/	/
Elongation rate of lateral roots (cm/day)	■	■	■	■	■	■				***	NA	NS	***	***	***	/	/	/

Figure 13 illustrates the effect of N availability on the morphological and physiological traits measured across the maize varieties. Throughout the following description, the 0.5 N treatment is referred to as low N (LN) and the 3 N treatment as moderate low N (MLN). The present section focuses primarily on overall trait responses to N limitation across all varieties. Differences among

variety groups (high-efficiency landraces, low-efficiency landraces and hybrids) are examined separately in the following sections.

N availability strongly affected plant biomass production. Both root and shoot dry weights decreased with increasing N limitation, with the reduction being particularly pronounced for shoot biomass (A, C). Consequently, the root-to-shoot ratio increased under LN across all varieties, indicating a greater relative investment in root development when N availability was limited (E).

Plant water status also responded to N availability. Root and shoot water contents were generally higher under MLN than under LN (B, D).

Leaf chlorophyll status differed markedly between treatments. SPAD values measured at day 0 were generally higher under MLN, suggesting a higher leaf chlorophyll content and potentially a better N status (F). In contrast, SPAD differences were mostly positive under LN and close to zero or negative under MLN (G).

Changes in most architectural root traits were less pronounced than those observed for biomass-related traits. The number of SR and LR angle varied little between treatments, whereas SR angle tended to increase slightly under stronger N limitation (H–J).

The response of root growth dynamics was more variable. No consistent treatment effect was detected for SR elongation rate when data from both replicates were combined, likely because opposite trends were observed between replicates (K). In contrast, LR elongation rate and LR density were generally greater under MLN (L, M). Finally, the duration of primordium development tended to be slightly longer under LN, suggesting a delay in LR emergence under stronger N limitation (N).

Taken together, these results indicate that N limitation primarily affected plant biomass production, chlorophyll status and LR elongation and density, whereas most architectural root traits remained comparatively stable across treatments.

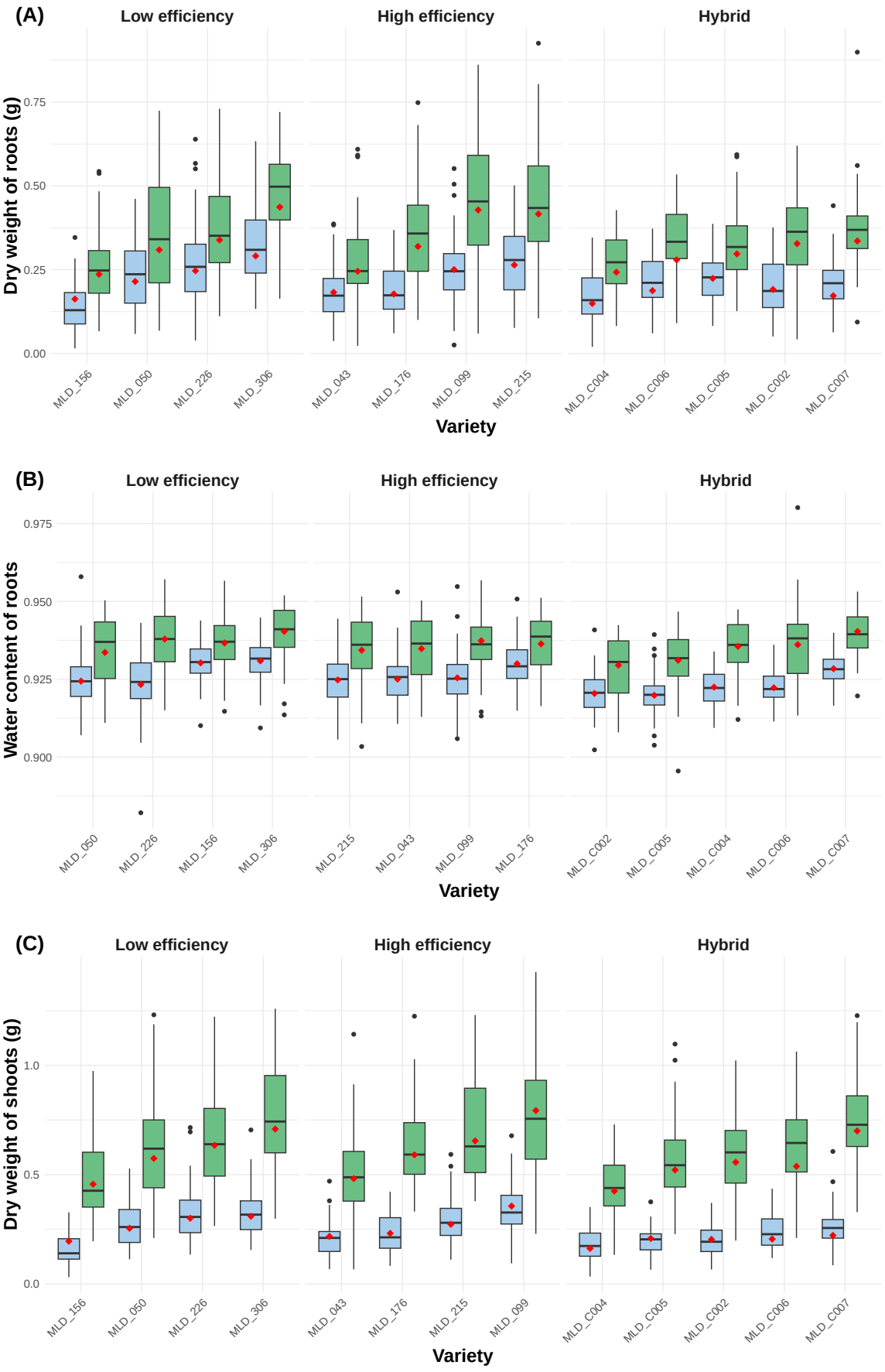
(A)
Low efficiency
High efficiency
Hybrid
Dry weight of roots (g)
0.00
0.25
0.50
0.75
MLD_156
MLD_050
MLD_226
MLD_306
MLD_043
MLD_176
MLD_099
MLD_215
MLD_C004
MLD_C006
MLD_C005
MLD_C002
MLD_C007
Variety
(B)
Low efficiency
High efficiency
Hybrid
Water content of roots
0.900
0.925
0.950
0.975
MLD_050
MLD_226
MLD_156
MLD_306
MLD_215
MLD_043
MLD_099
MLD_176
MLD_C002
MLD_C005
MLD_C004
MLD_C006
MLD_C007
Variety
(C)
Low efficiency
High efficiency
Hybrid
Dry weight of shoots (g)
0.0
0.5
1.0
MLD_156
MLD_050
MLD_226
MLD_306
MLD_043
MLD_176
MLD_215
MLD_099
MLD_C004
MLD_C005
MLD_C002
MLD_C006
MLD_C007
Variety

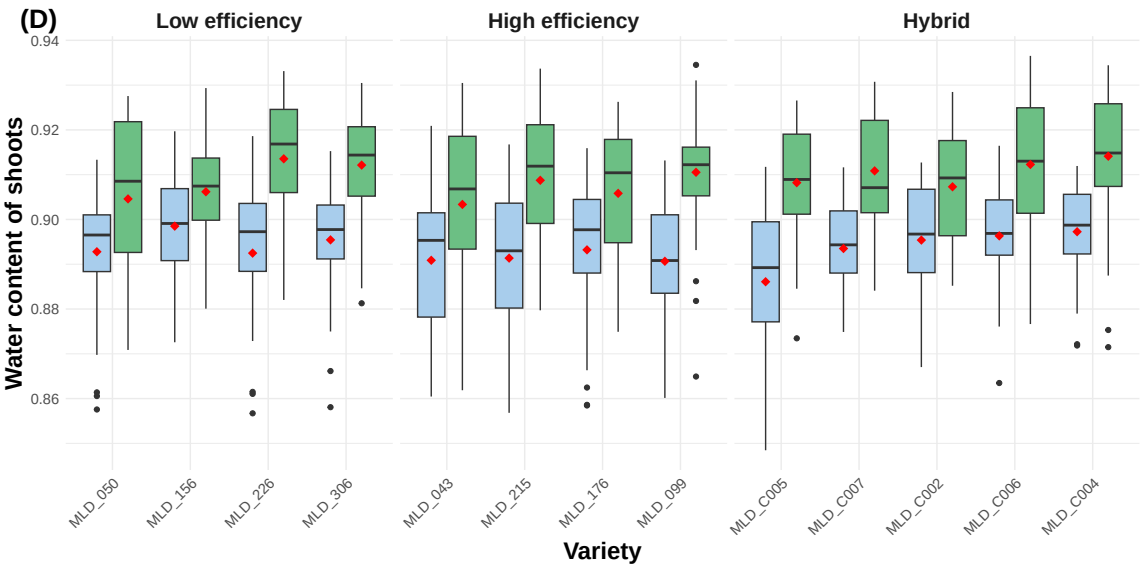
(D)
Low efficiency
High efficiency
Hybrid
Water content of shoots
0.94
0.92
0.90
0.88
0.86
MLD_050
MLD_156
MLD_226
MLD_306
MLD_043
MLD_215
MLD_176
MLD_099
MLD_C005
MLD_C007
MLD_C002
MLD_C006
MLD_C004
Variety

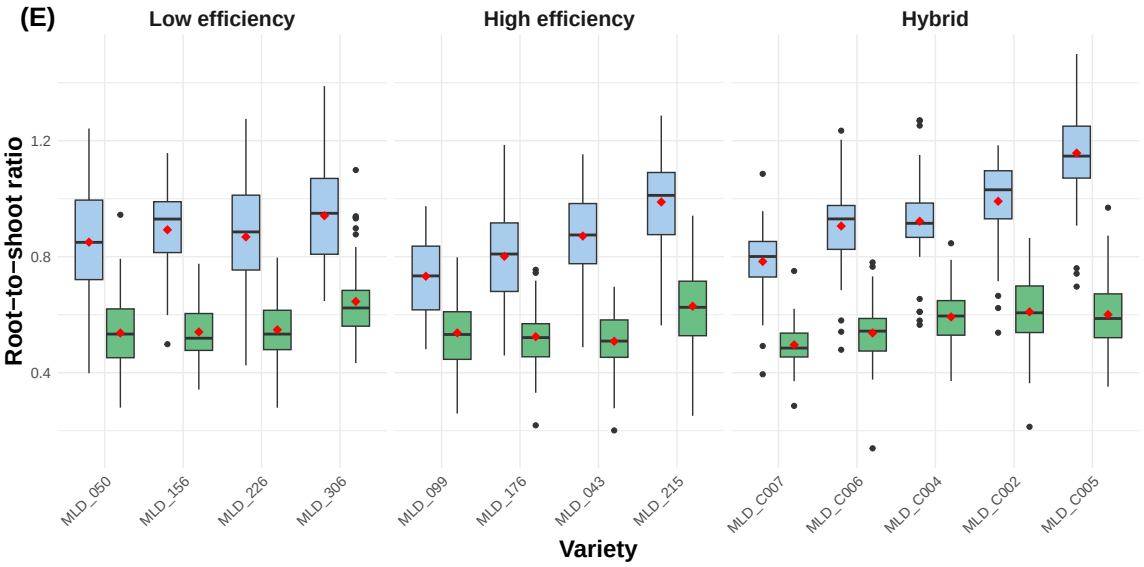
(E)
Low efficiency
High efficiency
Hybrid
Root−to−shoot ratio
1.2
0.8
0.4
MLD_050
MLD_156
MLD_226
MLD_306
MLD_099
MLD_176
MLD_043
MLD_215
MLD_C007
MLD_C006
MLD_C004
MLD_C002
MLD_C005
Variety

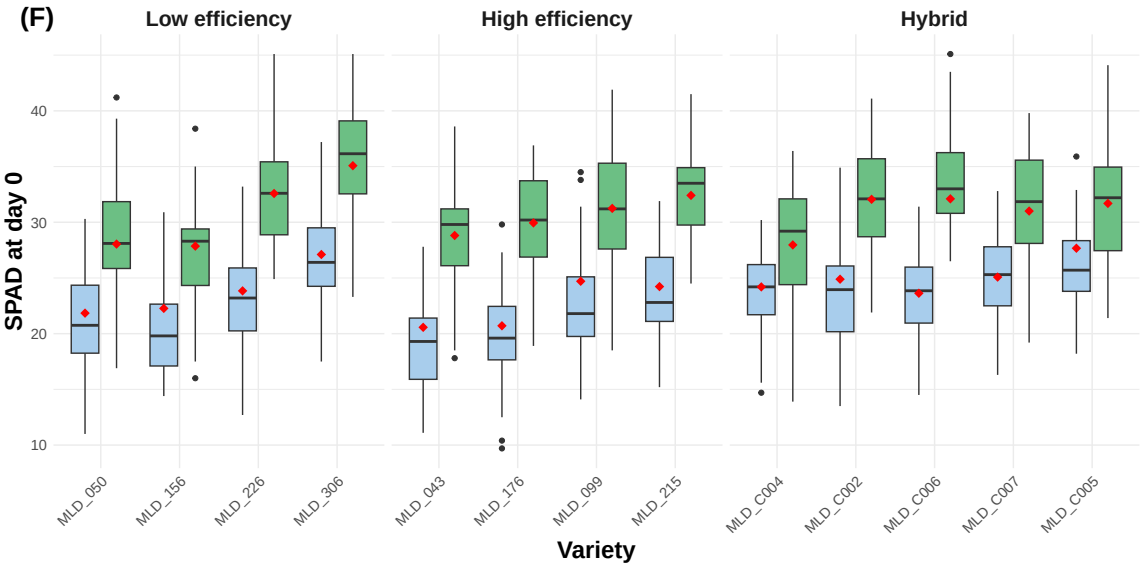
(F)
Low efficiency
High efficiency
Hybrid
SPAD at day 0
40
30
20
10
MLD_050
MLD_156
MLD_226
MLD_306
MLD_043
MLD_176
MLD_099
MLD_215
MLD_C004
MLD_C002
MLD_C006
MLD_C007
MLD_C005
Variety

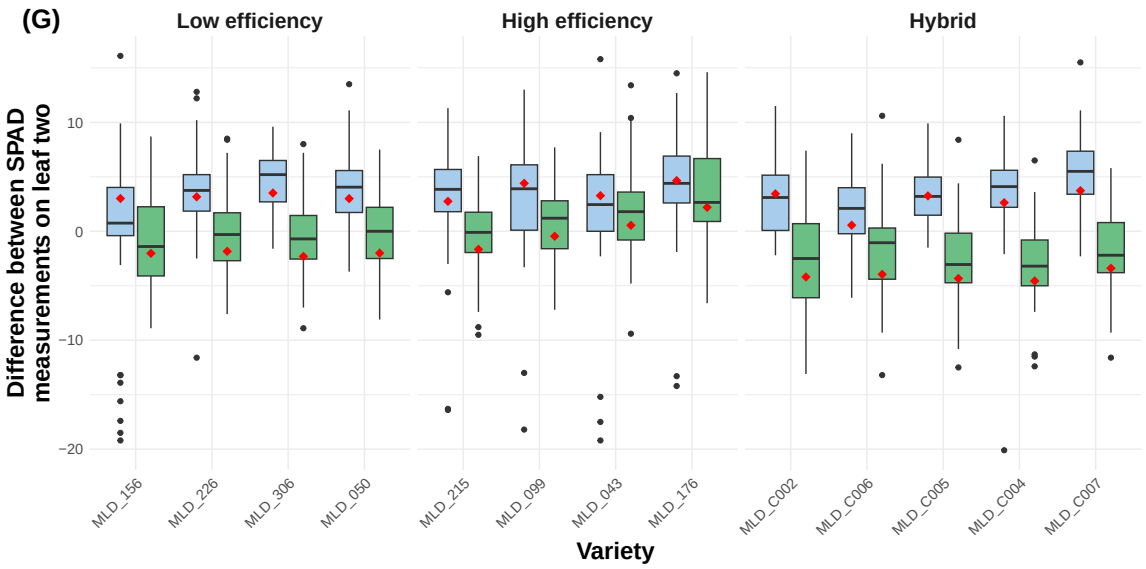
(G)
Low efficiency
High efficiency
Hybrid
Difference between SPAD measurements on leaf two
10
0
−10
−20
MLD_156
MLD_226
MLD_306
MLD_050
MLD_215
MLD_099
MLD_043
MLD_176
MLD_C002
MLD_C006
MLD_C005
MLD_C004
MLD_C007
Variety

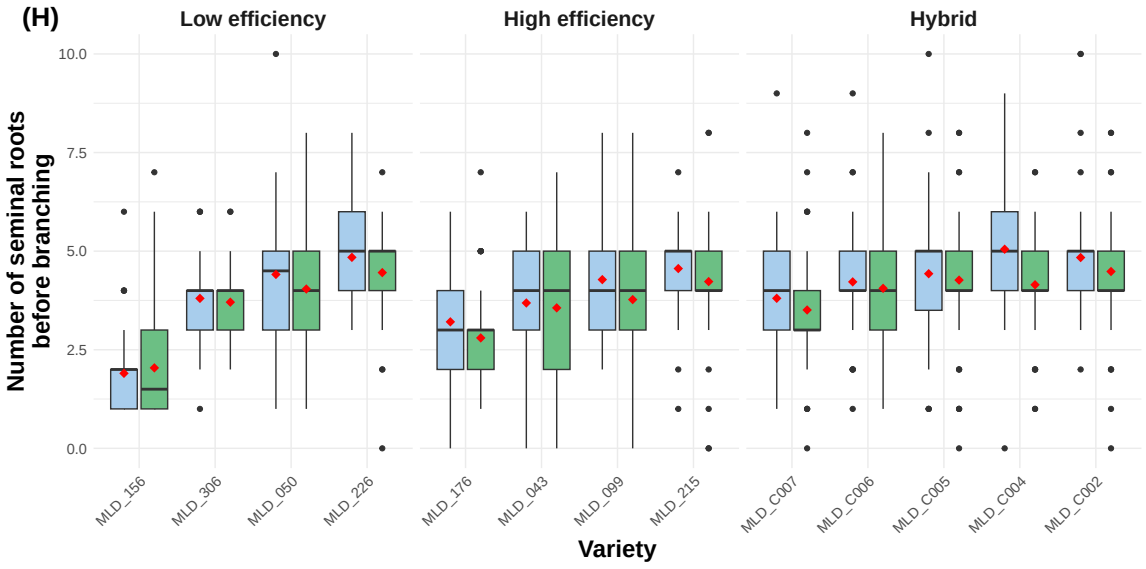
(H)
Low efficiency
High efficiency
Hybrid
Number of seminal roots before branching
10.0
7.5
5.0
2.5
0.0
MLD_156
MLD_306
MLD_050
MLD_226
MLD_176
MLD_043
MLD_099
MLD_215
MLD_C007
MLD_C006
MLD_C005
MLD_C004
MLD_C002
Variety

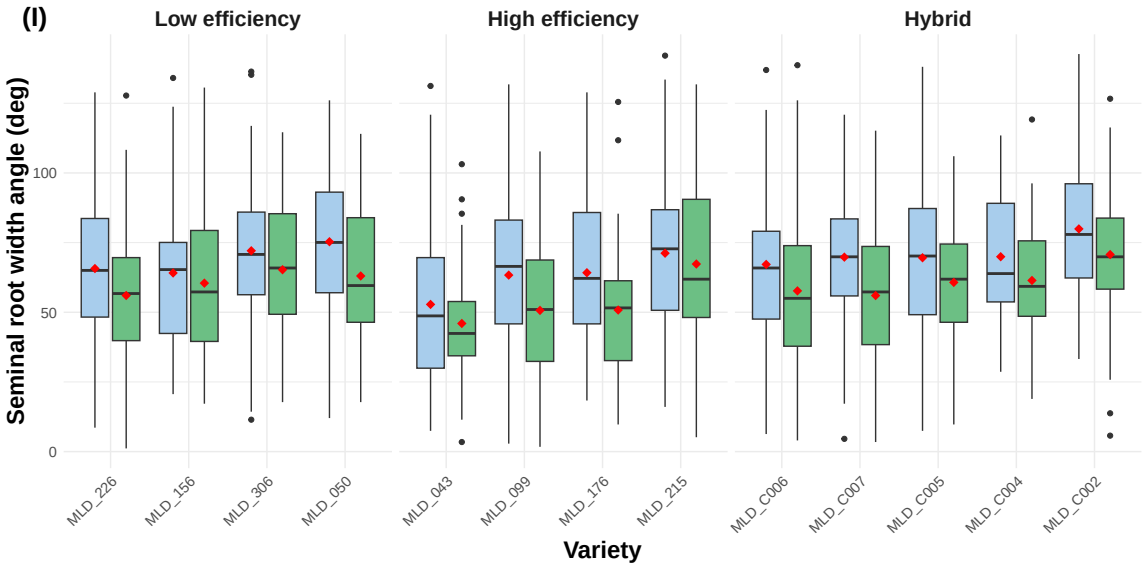
(I)
Low efficiency
High efficiency
Hybrid
Seminal root width angle (deg)
100
50
0
MLD_226
MLD_156
MLD_306
MLD_050
MLD_043
MLD_099
MLD_176
MLD_215
MLD_C006
MLD_C007
MLD_C005
MLD_C004
MLD_C002
Variety

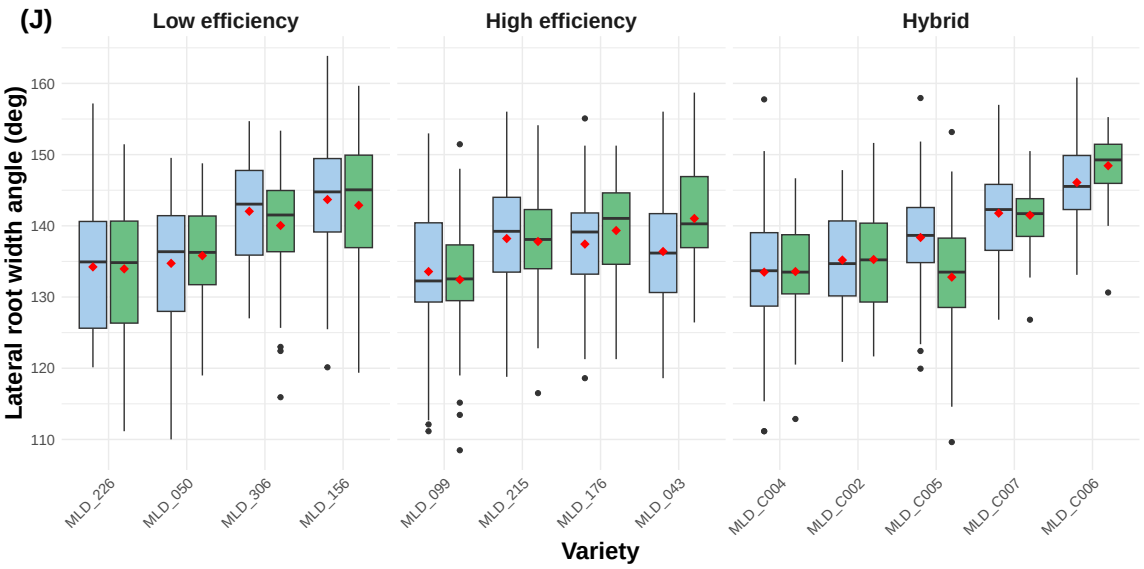
(J)
Low efficiency
High efficiency
Hybrid
Lateral root width angle (deg)
160
150
140
130
120
110
MLD_226
MLD_050
MLD_306
MLD_156
MLD_099
MLD_215
MLD_176
MLD_043
MLD_C004
MLD_C002
MLD_C005
MLD_C007
MLD_C006
Variety

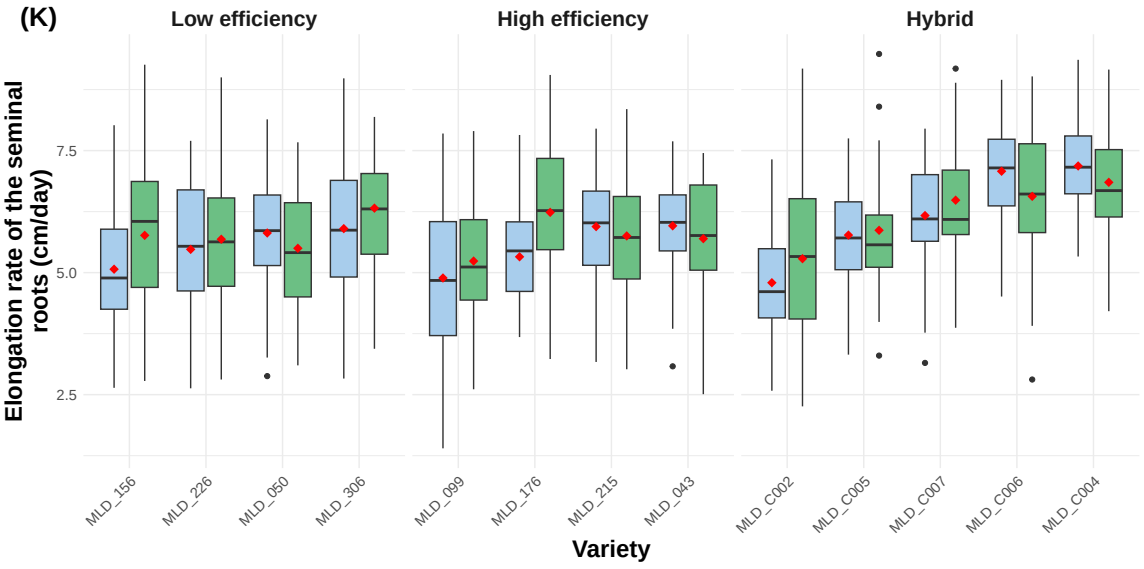
(K)
Low efficiency
High efficiency
Hybrid
Elongation rate of the seminal roots (cm/day)
7.5
5.0
2.5
MLD_156
MLD_226
MLD_050
MLD_306
MLD_099
MLD_176
MLD_215
MLD_043
MLD_C002
MLD_C005
MLD_C007
MLD_C006
MLD_C004
Variety

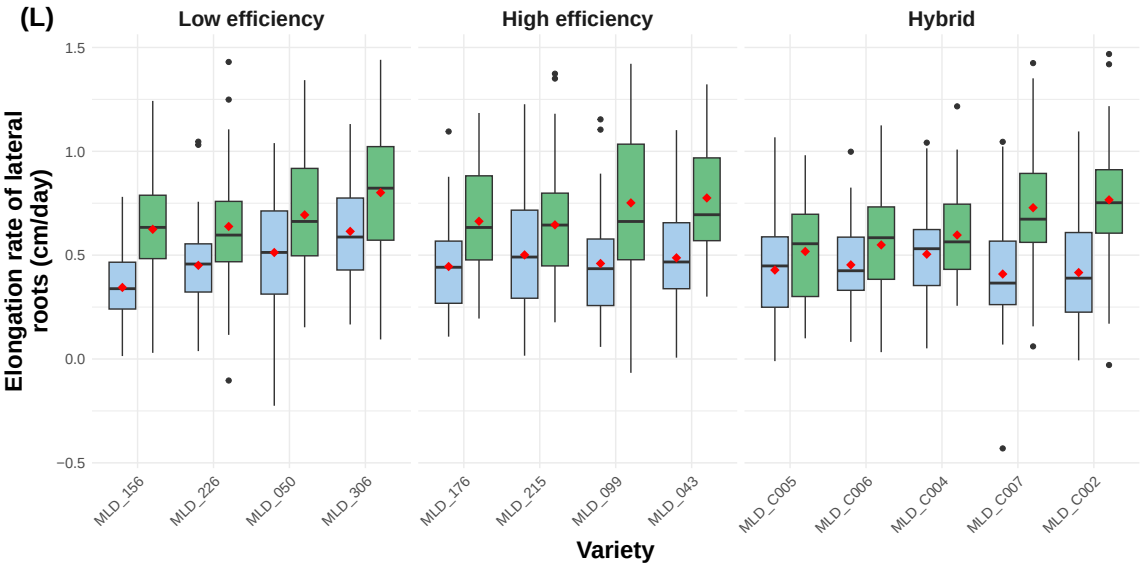
(L)
Low efficiency
High efficiency
Hybrid
Elongation rate of lateral roots (cm/day)
1.5
1.0
0.5
0.0
−0.5
MLD_156
MLD_226
MLD_050
MLD_306
MLD_176
MLD_215
MLD_099
MLD_043
MLD_C005
MLD_C006
MLD_C004
MLD_C007
MLD_C002
Variety

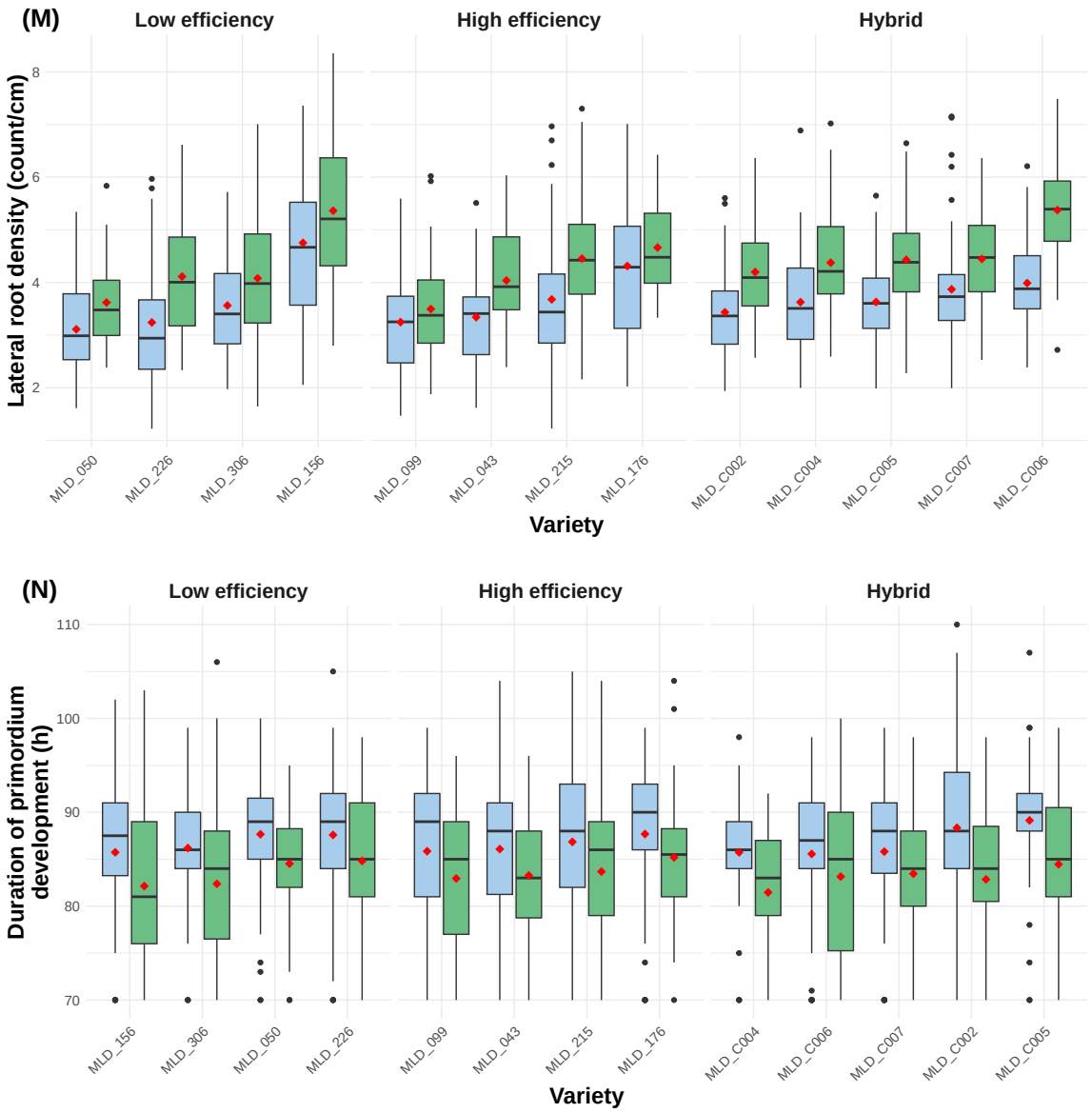

Figure 13: **Effect of nitrogen treatment on morphological and physiological traits of maize varieties.** (A) Root dry weight, (B) Root water content, (C) Shoot dry weight, (D) Shoot water content, (E) Root-to-shoot ratio, (F) SPAD value at day 0, (G) SPAD difference, (H) Seminal root number, (I) Seminal root angle, (J) Lateral root angle, (K) Seminal root elongation rate, (L) Lateral root elongation rate, (M) Lateral root density, (N) Duration of primordium development. Blue boxplots correspond to N treatment = 0.5mM and green boxplots correspond to N treatment = 3mM. Red diamonds represent estimated marginal means from the mixed models.

5.2.2 Phenotypic plasticity

Trait-specific plasticity

Phenotypic plasticity was assessed by comparing the model-estimated trait values obtained under MLN and LN . Figure 14 illustrates these relationships for all measured traits. For each trait, the position of a point is determined by the estimated value of a variety under 3 N (x-axis) and 0.5 N (y-axis). Points located close to the diagonal indicate limited changes between N treatments,

whereas points located further from the diagonal reflect stronger plastic responses.

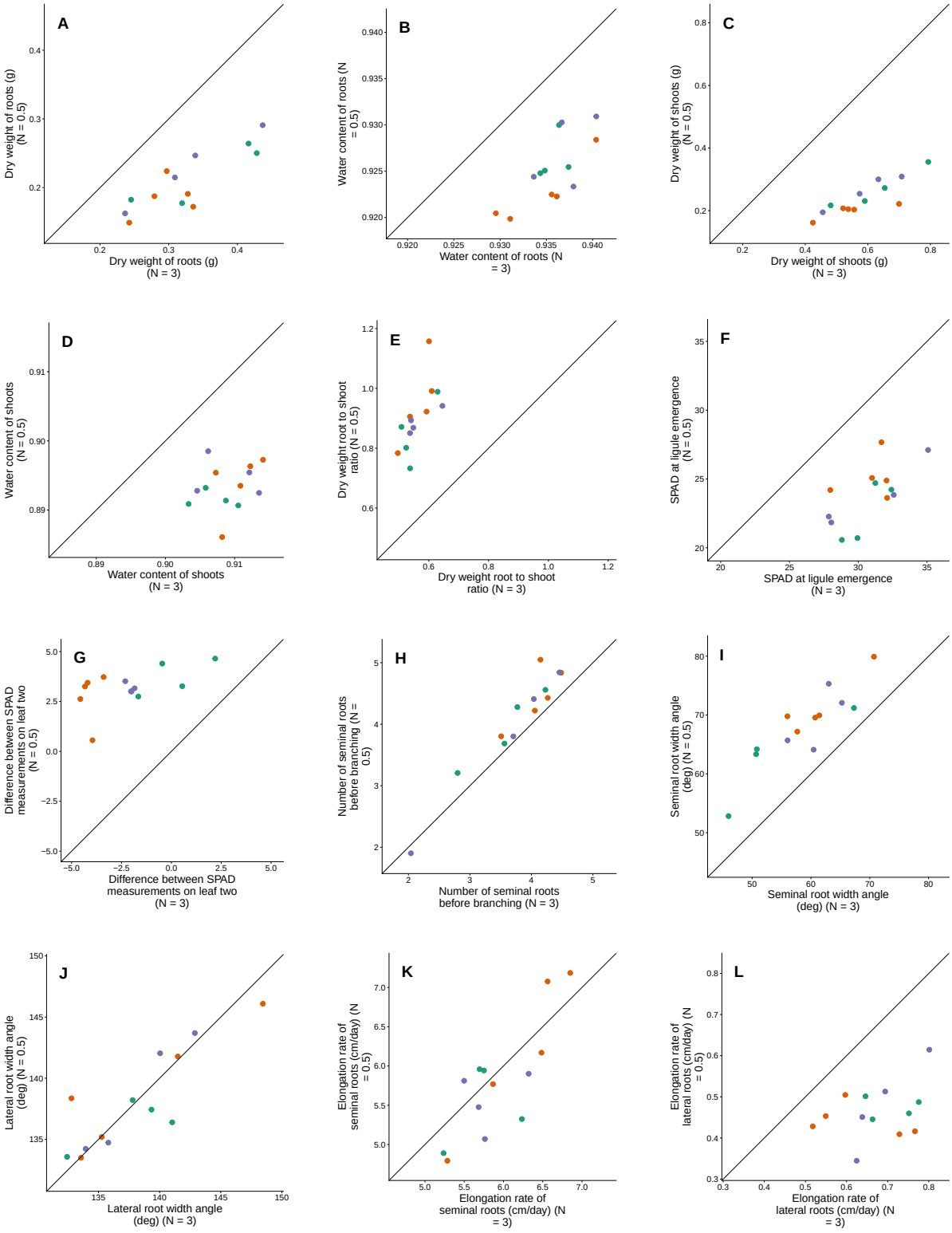

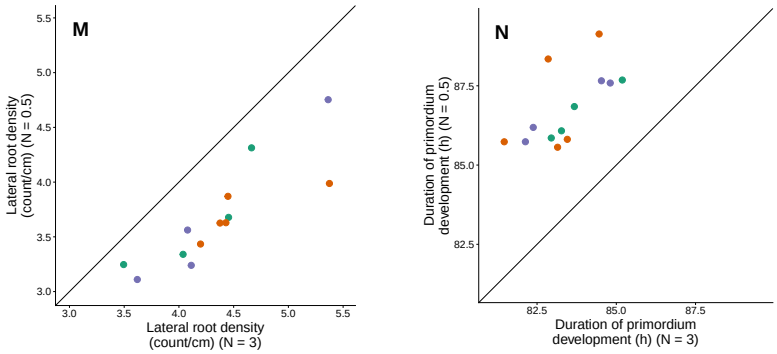

Figure 14: **Plastic response of measured traits between moderate low nitrogen (3 N) and severe low nitrogen (0.5 N).** Each point represents one variety. The diagonal line indicates equal trait values under both nitrogen treatments. (A) Root dry weight, (B) Root water content, (C) Shoot dry weight, (D) Shoot water content, (E) Root-to-shoot ratio, (F) SPAD value at ligule emergence, (G) SPAD difference, (H) Seminal root number, (I) Seminal root angle, (J) Lateral root angle, (K) Seminal root elongation rate, (L) Lateral root elongation rate, (M) Lateral root density, (N) Duration of primordium development. Hybrid varieties are shown in orange, high-efficiency landraces in green, and low-efficiency landraces in blue.

Figure 14 reveals contrasting levels of phenotypic plasticity among traits. Biomass-related traits showed the strongest responses to N limitation, with most points located well below the diagonal for root and shoot dry weight, indicating consistent reductions under N limitation. In contrast, the root-to-shoot ratio increased in all varieties, as illustrated by points positioned above the diagonal.

Table 3: **Mean relative change (%) of measured traits between moderate low nitrogen (3 N) and severe low nitrogen (0.5 N).** Negative values indicate a decrease under severe nitrogen limitation, whereas positive values indicate an increase.

Trait	Mean change (%)	SD (%)
Root dry weight	-35.15	7.53
Root water content	-1.12	0.27
Shoot dry weight	-59.03	4.29
Shoot water content	-1.72	0.46
Root-to-shoot ratio	60.22	13.40
SPAD at ligule emergence	-22.42	5.37
Number of seminal roots before branching	7.60	6.85
Seminal root angle	15.98	6.63
Lateral root angle	0.05	1.75
Seminal root elongation rate	-2.54	7.29
Lateral root elongation rate	-30.35	10.95
Lateral root density	-15.45	5.24
Duration of primordium development	4.05	1.17

While Figure 14 provides a visual assessment of the magnitude and consistency of trait responses to reduced N, Table 3 quantifies the average relative changes observed across varieties. Shoot dry weight decreased by nearly 60%, root dry weight by 35%, whereas the root-to-shoot ratio increased by approximately 60%. SPAD values at ligule emergence also declined substantially

(−22.4%). Among root traits, LR elongation rate and LR density exhibited the strongest reductions, decreasing by 30.4% and 15.5%, respectively.

Several architectural traits displayed smaller responses to N limitation than biomass-related traits. SR angle and the number of SR before branching increased moderately under severe N limitation, whereas LR angle remained largely unchanged. However, the direction of these responses was not always consistent among genotypes, with some varieties showing slightly higher values under MLN and others under MLN.

Root and shoot water content, as well as the duration of primordium development, were among the least plastic traits. Their low average relative changes and small standard deviations indicate that these traits remained comparatively stable across N treatments and showed little variation in plastic responses among genotypes.

Relative changes were not calculated for SPAD difference because values were centered around zero, making percentage changes difficult to interpret.

Plasticity differences among variety groups

Because NUE was the main criterion used to classify the landraces, we next examined whether the magnitude and direction of plastic responses differed among high-efficiency landraces, low-efficiency landraces and hybrids.

Mean relative plasticity differed more strongly among traits than among variety groups (Figure 15). Across all groups, the largest responses to N limitation were observed for shoot dry weight, root dry weight, root-to-shoot ratio and LR elongation rate. In contrast, root and shoot water content, LR angle and SR elongation rate exhibited only minor changes under reduced N availability.

Although the overall patterns were broadly similar among groups, some differences in the magnitude of plastic responses were observed. Hybrids tended to show stronger reductions in shoot dry weight and larger increases in root-to-shoot ratio, although differences among groups remained modest relative to differences among traits

Overall, variation in plasticity appeared to be more strongly associated with the phenotypic trait considered than with the predefined variety groups.

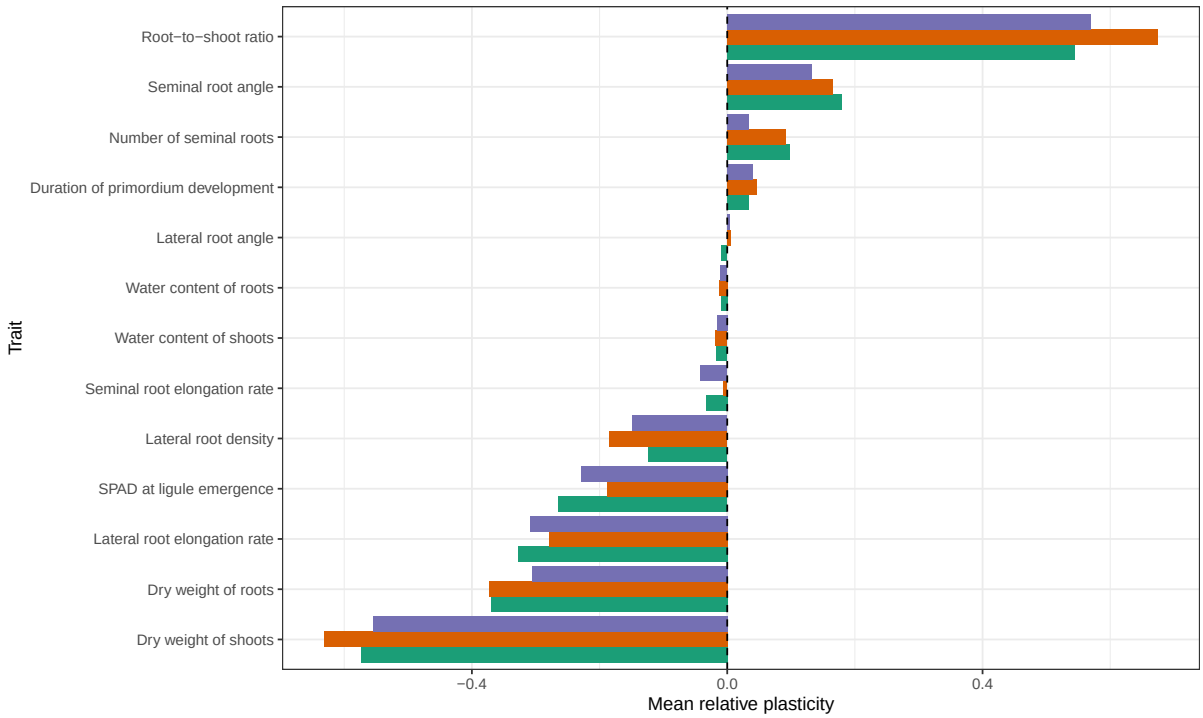

Figure 15: **Mean relative plasticity of morphological and physiological traits in response to nitrogen limitation for the three variety groups.** Relative plasticity was calculated as (LowN – HighN)/HighN, where negative values indicate a decrease and positive values an increase under severe nitrogen limitation (0.5 N) relative to moderate low nitrogen conditions (3 N). Bars represent the mean plasticity of each group across varieties. High-efficiency varieties are shown in green, low-efficiency varieties in purple, and hybrids in orange.

5.2.3 Multivariate analysis of plasticity

Given the marked differences in plasticity among traits and the variability observed among genotypes, a principal component analysis was performed on the plasticity indices to identify the main axes of variation and determine whether coordinated patterns of plastic responses emerged across genotypes.

Principal component analysis

The first two principal components (PC) explained 47.4% of the total variation in trait plasticity, with PC1 and PC2 accounting for 26.2% and 21.2% of the variance, respectively (Figure 16 A).

Several biomass-related traits, including root dry weight (DWR), shoot dry weight (DWS) and root-to-shoot ratio (DWRS), were positively associated with PC1 and clustered closely together, indicating coordinated plastic responses among biomass traits. Varieties exhibiting strong plasticity for one biomass trait therefore tended to show similar responses for the others.

Root water content (WCR) and shoot water content (WCS) were primarily associated with positive values of PC2, whereas SPAD at ligule emergence (S_d0l), SR angle (a_{SR}), number

of SR before branching (c_{SR}) and LR angle (a_{LR}) were associated with negative values of PC2. This pattern suggests that water-related traits and several architectural traits responded independently to N limitation.

Several root architectural traits were distributed on opposite sides of the PCA space. LR density (d_{LR}) was negatively associated with PC1, whereas SR elongation rate (e_{SR}) and LR elongation rate (e_{LR}) were positively associated with this axis. This opposition suggests contrasting plastic responses between root branching and root elongation processes. In practical terms, genotypes exhibiting strong plasticity in LR density tended to show lower plasticity in both SR and LR elongation rates, whereas genotypes displaying greater plasticity in root elongation generally showed weaker plasticity in LR density. This pattern may reflect a trade-off in the allocation of resources between the production of LRs and the elongation of existing root axes under contrasting N conditions.

The PCA of individuals (16B) showed substantial overlap among the three variety groups on the first two principal components. No distinct clustering pattern was observed, indicating that plasticity responses varied more among genotypes within groups than between the predefined variety groups.

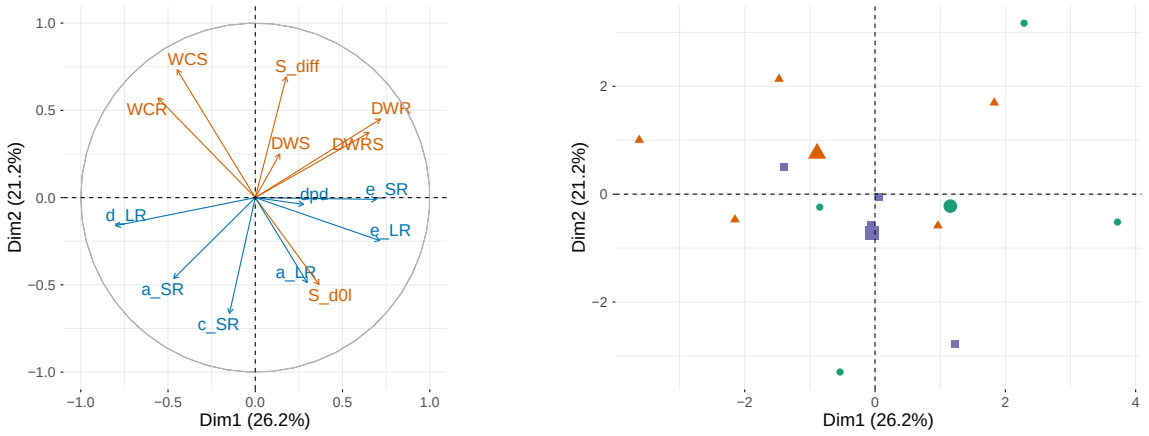

(a) Correlation circle

(b) Individual factor map

Figure 16: **Principal component analysis (PCA) performed using the plasticity indices of all measured traits.** (A) Correlation circle showing the relationships between trait plasticity variables. Root architectural traits are shown in blue and biomass/physiological traits in orange. (B) Projection of genotypes on the first two principal components. Hybrids are shown in orange, high-efficiency landraces in green and low-efficiency landraces in blue. Abbreviations: DWR, root dry weight; WCR, root water content; DWS, shoot dry weight; WCS, shoot water content; DWRS, root-to-shoot ratio; S_d0l, SPAD at ligule emergence; S_diff, difference between SPAD measurements; a_{SR}, seminal root angle; a_{LR}, lateral root angle; c_{SR}, number of seminal roots before branching; e_{SR}, seminal root elongation rate; d_{LR}, lateral root density; DPD, duration of primordium development; e_{LR}, lateral root elongation rate.

Relationships among plasticity traits

The correlation matrix (Figure 17) confirmed the relationships observed in the PCA. Plasticity in root dry weight (DWR) was positively correlated with plasticity in shoot dry weight (DWS;

$r = 0.66$) and root-to-shoot ratio (DWRS; $r = 0.58$), indicating coordinated variation among biomass-related traits. Similarly, plasticity in root water content (WCR) was positively correlated with plasticity in shoot water content (WCS; $r = 0.73$) and LR density (d_{LR}; $r = 0.60$).

Among root architectural traits, plasticity in LR density (d_{LR}) was negatively correlated with plasticity in SR elongation rate (e_{SR}; $r = -0.65$). In contrast, SR elongation rate (e_{SR}) was positively correlated with LR elongation rate (e_{LR}; $r = 0.62$). These relationships suggest that genotypes displaying strong plasticity in root elongation tended to exhibit lower plasticity in LR density.

Additional positive correlations were observed between SPAD at ligule emergence (S_d0l) and LR angle (a_{LR}; $r = 0.70$), as well as between SPAD at ligule emergence and duration of primordium development (DPD; $r = 0.57$), indicating that these traits tended to vary together in response to N limitation.

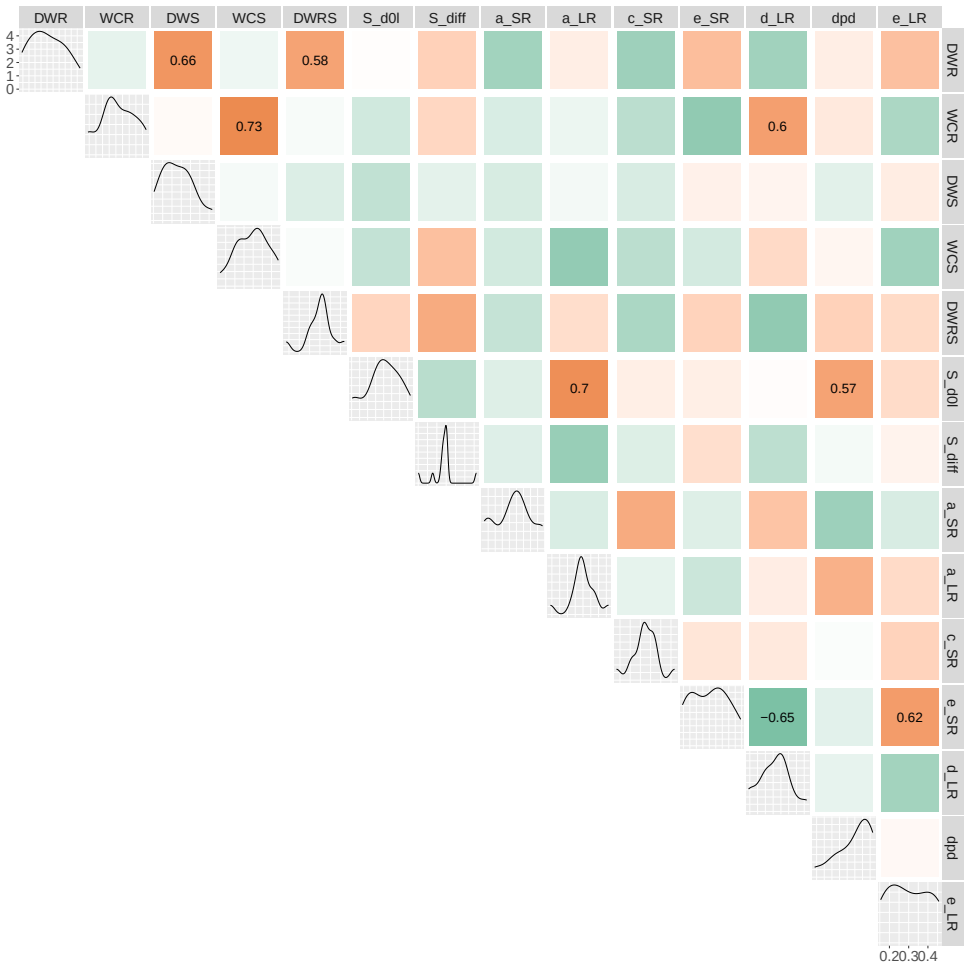

Figure 17: **Correlation matrix of relative phenotypic plasticity among morphological and physiological traits measured in maize varieties under contrasting nitrogen availability.** Relative plasticity was calculated as (LowN − HighN)/HighN. The diagonal panels show the distribution of plasticity values for each trait. Colored cells represent Pearson correlation coefficients between traits, with orange indicating positive correlations and green indicating negative correlations. Correlation coefficients are displayed only when significant ($p<0.05$). Abbreviations: DWR, root dry weight; WCR, root water content; DWS, shoot dry weight; WCS, shoot water content; DWRS, root-to-shoot ratio; S_d0l, SPAD at ligule emergence; S_diff, difference between SPAD measurements; a_{SR}, seminal root angle; a_{LR}, lateral root angle; c_{SR}, number of seminal roots before branching; e_{SR}, seminal root elongation rate; d_{LR}, lateral root density; DPD, duration of primordium development; e_{LR}, lateral root elongation rate.

6 Discussion

Response of root and physiological traits to N limitation

The reduction in biomass under LN conditions was more pronounced for shoot dry weight than for root dry weight. As a consequence, the R:S ratio increased under low N availability. This response is consistent with previous studies (Gao et al., 2015; Hermans et al., 2006) showing that N deficiency promotes a greater allocation of biomass to the root system at the expense of shoot growth. Such a shift in biomass allocation is generally interpreted as an adaptive strategy allowing plants to increase soil exploration and improve N acquisition under nutrient-limiting conditions.

Root and shoot water contents were generally higher under the MLN treatment than under LN. In addition, hybrid varieties exhibited lower root water content than landraces under both N conditions, whereas no clear group effect was observed for shoot water content. These results suggest differences in root physiological responses between hybrids and landraces, although the functional significance of this pattern remains unclear.

SPAD values measured at the beginning of the experiment were higher under MLN than under LN, indicating a higher chlorophyll content and therefore a better N status of the leaves. However, the evolution of SPAD values during the experiment differed between treatments. Under LN, SPAD differences were generally positive, indicating a decline in chlorophyll content over time and suggesting remobilization of N from leaves towards other organs. In contrast, SPAD differences under MLN were closer to zero or even negative, particularly in hybrids, indicating that chlorophyll levels were maintained or increased throughout the experiment. This pattern suggests that plants supplied with sufficient N continued investing in leaf function and photosynthetic capacity. The stronger maintenance of chlorophyll content observed in hybrids may reflect differences in N allocation strategies, although additional physiological measurements would be required to confirm this interpretation.

The response of SR angle to N treatment was relatively modest, with a tendency towards wider angles under LN conditions. However, this result should be interpreted cautiously because SR angle was measured at an early developmental stage, after only a short exposure to the N treatments. Furthermore, the interaction between variety and N treatment was not significant (Table 2), indicating that genotypes responded similarly to N availability for this trait.

According to the root ideotype proposed by Lynch, steeper SR angles may favour nitrate acquisition by promoting deeper rooting and access to mobile nitrate that has migrated to deeper soil layers (J. P. Lynch, 2013). However, the relevance of this strategy depends strongly on the

spatial and temporal distribution of N in the soil. Modelling studies by Dunbabin et al. demonstrated that when nitrate originates primarily from surface mineralization and is not continuously replenished through fertilization, rapid exploitation of the topsoil may be as effective as deep rooting. Under such conditions, dense root systems located near the soil surface can efficiently capture N before it is lost through leaching. Consequently, the absence of narrower SR angles under low N in the present study does not necessarily contradict current theories of N foraging but rather highlights that optimal root architecture depends on the environmental context.

No consistent effect of N treatment was observed on SR elongation rate when both replicates were analysed together. However, when analysed separately, replicate 1 showed a tendency for higher elongation rates under MLN than under LN, although this pattern was not observed for all varieties. In contrast, no clear trend emerged from replicate 2. Interpretation of these results is complicated by the accidental water deficit that occurred during the second replicate. The interruption of irrigation temporarily stopped primary root growth, resulting in elongation measurements being performed on SRs rather than on the primary root as initially intended. Consequently, direct comparison between replicates should be approached with caution and further analyses would be required to better understand the effect of this event on root growth dynamics.

In contrast, LR traits exhibited clearer responses to N availability. Both LR density and LR elongation rate were higher under MLN than under LN. These results indicate that plants supplied with sufficient N invested more resources in the development and expansion of LRs. Under severe N limitation, reduced N availability likely constrained the growth of LRs. Rather than indicating an absence of plasticity, these responses reveal an active adjustment of root developmental processes to nutrient availability. The coordinated reduction in both LR density and elongation rate under LN suggests that N availability strongly influences the capacity of maize seedlings to deploy LRs and explore the surrounding environment. From an energetic perspective, this response may also represent a resource-conservation strategy. When N availability is extremely low, investing heavily in the production of new LRs may provide limited returns in terms of nutrient acquisition. Reducing LR development could therefore allow plants to limit construction and maintenance costs while preserving resources for other essential functions.

Finally, the duration of primordium development was generally longer under LN conditions, indicating that LR emergence was delayed when N availability was reduced. One possible explanation is that reduced N supply decreases metabolic activity and resource transport within the root system, thereby slowing the developmental processes leading to LR emergence.

Beyond the individual responses of each trait, the overall pattern observed under N limitation highlights that maize seedlings adjusted several components of their root system in response to reduced N availability. These adjustments did not follow a single predefined root ideotype but instead involved coordinated modifications of multiple developmental processes. While SR angles and elongation rates remained relatively stable, LR development was affected, with

reduced density, slower elongation and delayed emergence under LN conditions. At the same time, plants increased their R:S ratio, indicating a greater relative investment in belowground structures.

This combination of responses does not support a clear shift towards either the "Topsoil Foraging" or the "Steep, Cheap and Deep" ideotype. Instead, it suggests that young maize plants respond to N limitation through a balance between maintaining soil exploration capacity and reducing the metabolic costs associated with root construction. More generally, these results support the view that adaptation to N limitation relies on the integration of multiple root and physiological traits rather than on the modification of a single architectural characteristic, as emphasized by functional-structural approaches developed by Dunbabin and colleagues.

Phenotypic plasticity and coordinated trait responses

The magnitude of phenotypic plasticity differed considerably among traits. Biomass-related traits displayed the strongest responses to N limitation, particularly shoot dry weight and the R:S ratio, whereas most root architectural traits remained comparatively stable. Among RSA traits, LR density, LR elongation rate and primordium development duration showed the greatest plasticity, highlighting the particular sensitivity of LR development to N availability.

Despite these trait-specific responses, differences in plasticity among the predefined groups were relatively small. High-efficiency landraces, low-efficiency landraces and hybrids generally responded in the same direction to N limitation, although the magnitude of the response varied among individual varieties. This pattern was further supported by the PCA of plasticity values, which did not reveal a clear separation among groups.

The multivariate analyses nevertheless revealed coordinated patterns of trait responses. Biomass-related traits tended to vary together, suggesting common physiological mechanisms underlying their plasticity. In contrast, LR density was negatively associated with root elongation traits, indicating a possible trade-off between investment in LR production and root extension. Although the mechanisms underlying this relationship remain unclear, this pattern suggests that different genotypes may allocate available resources differently when responding to N limitation.

Relationship between NUE classification and root traits

Contrary to our initial expectations, only limited differences were observed between the high-efficiency and low-efficiency landrace groups. Most notably, high-efficiency and low-efficiency landraces could not be clearly distinguished based on the root and physiological traits measured in this study.

The model summary provides useful insight into this result. The interaction between group and N treatment was significant only for the R:S ratio and SPAD-related variables. These traits

therefore represent the only cases where the response to N availability differed among groups. For most other traits, groups differed in their average values independently of N treatment, but they responded to N limitation in a similar direction and with comparable magnitudes.

This distinction between baseline group differences and treatment responses is illustrated schematically in Figure 18.

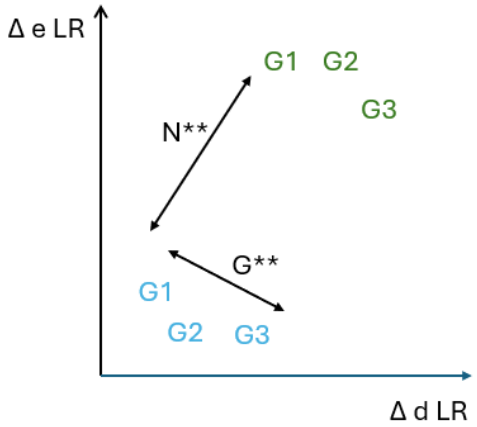

Figure 18: Conceptual illustration of the distinction between group effects and group-by-treatment interactions. Groups may differ in their average trait values independently of N availability (group effect), while still exhibiting similar responses to N limitation. A significant group-by-treatment interaction occurs only when groups respond differently to the N treatment.

While the group-level response to N limitation was generally similar, a different pattern emerged when examining individual varieties. Within each group, varieties often differed substantially in both trait values and plastic responses. Consequently, varieties belonging to the same NUE group did not necessarily exhibit similar responses to N limitation.

The distinction between group-level and variety-level responses is illustrated schematically in Figure 19.

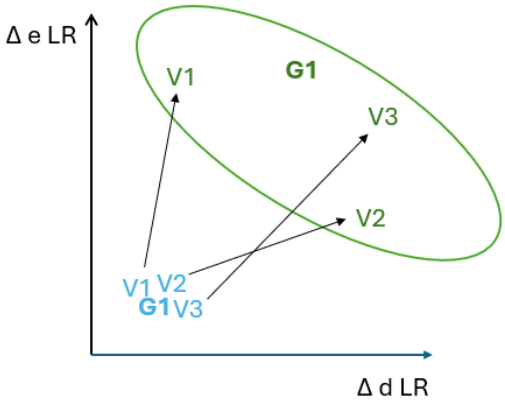

Figure 19: Conceptual illustration of the variety-by-treatment interaction. Although varieties belonging to the same NUE group may respond in the same overall direction to N limitation, the magnitude and combination of trait responses can differ substantially among varieties. Consequently, group membership alone does not necessarily predict the plastic response of individual genotypes.

Several hypotheses may explain the absence of clear differences between high- and low-efficiency landraces. First, all measurements were performed on young plants during the first three weeks of development. Differences associated with NUE may therefore become more apparent later in the life cycle, when nutrient demand increases and root systems are more developed. The developmental stage investigated here may not fully capture the mechanisms underlying NUE differences among landraces.

Second, the traits measured in this study may not correspond to the primary determinants of NUE. Although RSA is often considered an important component of adaptation to nutrient limitation, NUE is a complex trait integrating numerous physiological and developmental processes. N uptake efficiency depends not only on root architecture but also on physiological mechanisms involved in nutrient acquisition, including transporter activity and uptake capacity. Furthermore, NUE depends on the efficiency with which absorbed N is assimilated, remobilized and converted into biomass. Consequently, differences between high- and low-efficiency landraces may be more strongly associated with physiological mechanisms than with the early root architectural traits measured here.

More generally, NUE emerges from the interaction of multiple factors, including soil N availability, environmental conditions, crop management practices and genotype-specific responses (Congreves et al., 2021). The absence of clear differences in root traits between the two landrace groups therefore suggests that NUE variation results from a broader combination of mechanisms than those investigated in the present study. Future work integrating later developmental stages, physiological measurements and whole-plant N dynamics would help identify the traits responsible for the NUE differences previously reported among these landraces.

7 Conclusion

This study aimed to investigate the response of maize landraces and hybrids to N limitation by characterizing both root architectural and biomass-related traits on the RootPhAir platform. In particular, the study sought to determine whether maize landraces previously classified as high- or low-NUE genotypes under field conditions exhibited contrasting responses to N deficiency under controlled conditions and how these responses compared with those of modern hybrid varieties. N limitation strongly affected plant growth, resulting in a substantial reduction in biomass, particularly in shoot tissues. As a consequence, the R:S ratio increased under low N conditions, indicating a shift in resource allocation towards the root system. Several root traits also responded to N availability, although the magnitude of these responses was generally smaller than that observed for biomass-related traits. SR angles tended to be wider under low N conditions, suggesting a modest adjustment in root system spatial exploration. While SR elongation rate did not show a consistent response to N limitation, both LR density and LR elongation rate were generally reduced under low N conditions, indicating a reduced investment in LR development under severe N limitation. Together, these responses indicate that N deficiency influences not only plant growth but also the balance between root system expansion and LR development. The observed responses did not support the emergence of a clearly identifiable root ideotype under N limitation, suggesting that N acquisition efficiency may depend on complex interactions among multiple traits rather than on individual root characteristics considered in isolation. The comparison between the predefined variety groups did not reveal clear differences in their responses to N limitation. Landraces previously classified as high- or low-NUE did not exhibit distinct root architectural patterns or response strategies at the developmental stage investigated in this study. However, several traits showed consistent responses to N limitation across genotypes, including increased R:S ratio and reduced LR development. The absence of clear group differentiation suggests that variation among individual varieties within each group was greater than the average differences between groups. It is therefore possible that the mechanisms underlying NUE are expressed through genotype-specific combinations of traits or become more apparent at later developmental stages than those examined here. The analysis of phenotypic plasticity largely confirmed the patterns observed in the trait responses. Correlations between plasticity indices highlighted coordinated responses among several traits, particularly the negative relationship between LR density and root elongation rates, suggesting a potential trade-off between the production of LRs and the elongation of existing root axes. These results further support the view that adaptation to N limitation relies on coordinated adjustments among multiple traits rather than on large modifications of individual root characteristics. Overall, the results support the view that adaptation to N limitation involves coordinated adjustments among

multiple traits rather than major modifications of individual root architectural characteristics. While N limitation induced consistent responses across several traits, substantial variability was observed among genotypes. Importantly, variation among individual genotypes was often greater than variation between the predefined NUE groups, highlighting the complexity of the traits underlying N use efficiency and the importance of considering genotype-specific response strategies. However, the relatively young developmental stage investigated and the controlled conditions of the RootPhAir platform may have limited the expression of genotypic differences that contribute to NUE under field conditions. Future work should aim to validate these findings under field conditions, where root systems develop in a more complex and heterogeneous environment. Approaches such as shovelomics could be used to characterize mature RSA and determine whether the patterns observed during early development persist throughout the crop cycle and contribute to N uptake efficiency, biomass production and grain yield. Extending observations to later developmental stages and integrating physiological measurements related to N uptake and utilization would also provide a more comprehensive understanding of the mechanisms underlying NUE variation among genotypes. Finally, the experimental data generated in this study could be used to parameterize and test root models, allowing the evaluation of how different combinations of root traits influence N acquisition under contrasting environmental conditions. By comparing simulated and observed responses, such approaches could help identify root ideotypes most likely to improve N uptake and performance in low-input agricultural systems.

Bibliography

Awasthi, P., & Laxmi, A. (2021). Root architectural plasticity in changing nutrient availability. In *Rhizobiology: Molecular physiology of plant roots* (pp. 25–37). Springer.

Azeez, M. A., Adubi, A. O., & Durodola, F. A. (2018). Landraces and crop genetic improvement. In *Rediscovery of landraces as a resource for the future*. IntechOpen.

Bates, D., Mächler, M., Bolker, B., & Walker, S. (2015). Fitting linear mixed-effects models using lme4. *Journal of Statistical Software*, *67*(1), 1–48. https://doi.org/10.18637/jss.v067.i01

Blake, R. (2026, March 18). *The persian gulf oil crisis is a food crisis*. IPES-Food. https://ipes-food.org/the-persian-gulf-oil-crisis-is-a-food-crisis/

Casañas, F., Simó, J., Casals, J., & Prohens, J. (2017). Toward an evolved concept of landrace. *Frontiers in plant science*, *8*, 245305.

Cassman, K. G., Dobermann, A., & Walters, D. T. (2002). Agroecosystems, nitrogen-use efficiency, and nitrogen management. *AMBIO: A Journal of the Human Environment*, *31*(2), 132–140.

Congreves, K. A., Otchere, O., Ferland, D., Farzadfar, S., Williams, S., & Arcand, M. M. (2021). Nitrogen use efficiency definitions of today and tomorrow. *Frontiers in Plant Science*, *12*, 637108.

Coombes, N. (2020). *Digger: Digger design generator under correlation and blocking* [R package version 1.0.5]. http://nswdpibiom.org/austatgen/software

Craswell, E. (2021). Fertilizers and nitrate pollution of surface and ground water: An increasingly pervasive global problem. *SN Applied Sciences*, *3*(4), 518.

Dathe, A., Postma, J. A., Postma-Blaauw, M., & Lynch, J. (2016). Impact of axial root growth angles on nitrogen acquisition in maize depends on environmental conditions. *Annals of Botany*, *118*(3), 401–414.

DeBruin, J. L., Schussler, J. R., Mo, H., & Cooper, M. (2017). Grain yield and nitrogen accumulation in maize hybrids released during 1934 to 2013 in the us midwest. *Crop Science*, *57*(3), 1431–1446.

Dunbabin, V., Diggle, A., & Rengel, Z. (2003a). Is there an optimal root architecture for nitrate capture in leaching environments? *Plant, Cell & Environment*, *26*(6), 835–844.

Dunbabin, V., Rengel, Z., & Diggle, A. (2003b). Root architecture and nutrient capture-the complex riddle of what constitutes optimality of root form and function. *Innovative Soil-Plant Systems for Sustainable Agricultural Practices Eds. JM Lynch, JS Schepers and I Unver*, 2–16.

Dunbabin, V., Rengel, Z., & Diggle, A. (2004). Simulating form and function of root systems: Efficiency of nitrate uptake is dependent on root system architecture and the spatial and temporal variability of nitrate supply. *Functional Ecology*, *18*(2), 204–211.

FAO. (2025). *Inorganic fertilizers. 2002–2023*. FAO. https://doi.org/10.4060/cd5938en

Feldman, L. (1994). The maize root. In *The maize handbook* (pp. 29–37). Springer.

Fitter, A., Stickland, T., Harvey, M., & Wilson, G. (1991). Architectural analysis of plant root systems 1. architectural correlates of exploitation efficiency. *New phytologist*, *118*(3), 375–382.

Gao, K., Chen, F., Yuan, L., Zhang, F., & Mi, G. (2015). A comprehensive analysis of root morphological changes and nitrogen allocation in maize in response to low nitrogen stress. *Plant, cell & environment*, *38*(4), 740–750.

Hermans, C., Hammond, J. P., White, P. J., & Verbruggen, N. (2006). How do plants respond to nutrient shortage by biomass allocation? *Trends in plant science*, *11*(12), 610–617.

Hirel, B., Le Gouis, J., Ney, B., & Gallais, A. (2007). The challenge of improving nitrogen use efficiency in crop plants: Towards a more central role for genetic variability and quantitative genetics within integrated approaches. *Journal of experimental botany*, *58*(9), 2369–2387.

Hochholdinger, F., Woll, K., Sauer, M., & Dembinsky, D. (2004). Genetic dissection of root formation in maize (zea mays) reveals root-type specific developmental programmes. *Annals of botany*, *93*(4), 359–368.

Hochholdinger, F., & Zimmermann, R. (2008). Conserved and diverse mechanisms in root development. *Current opinion in plant biology*, *11*(1), 70–74.

Hodge, A., Robinson, D., Griffiths, B., & Fitter, A. (1999). Why plants bother: Root proliferation results in increased nitrogen capture from an organic patch when two grasses compete. *Plant, Cell & Environment*, *22*(7), 811–820.

Hölker, A. C., Mayer, M., Presterl, T., Bolduan, T., Bauer, E., Ordas, B., Brauner, P. C., Ouzunova, M., Melchinger, A. E., & Schön, C.-C. (2019). European maize landraces made accessible for plant breeding and genome-based studies. *Theoretical and Applied Genetics*, *132*(12), 3333–3345.

IPES-Food. (2025). *Du pétrole dans l'assiette: Rapport ipes-food*. IPES-Food. https://ipes-food.org/fr/rapport/du-petrole-dans-l-assiette/

Kandpal, G. (2021). Review on impact of chemical fertilizers on environment. *Int. J. Mod. Agric*, *10*(1), 758–763.

Kochhar, S., & Gujral, S. K. (2020). *Plant physiology: Theory and applications: Theory and applications*. Cambridge University Press.

Lalonde, S., Wipf, D., & Frommer, W. B. (2004). Transport mechanisms for organic forms of carbon and nitrogen between source and sink. *Annu. Rev. Plant Biol.*, *55*(1), 341–372.

Lê, S., Josse, J., & Husson, F. (2008). FactoMineR: A package for multivariate analysis. *Journal of Statistical Software*, *25*(1), 1–18. https://doi.org/10.18637/jss.v025.i01

Lengrand, S. (2026). *Dissecting the role of root plasticity to enhance nutrient use uptake* [Seminar presented at UCLouvain, Louvain-la-Neuve, Belgium].

Lenth, R. V. (2025). *Emmeans: Estimated marginal means, aka least-squares means* [R package version 1.11.2-8]. https://doi.org/10.32614/CRAN.package.emmeans

Lynch, J. (1995). Root architecture and plant productivity. *Plant physiology*, *109*(1), 7.

Lynch, J. P. (2013). Steep, cheap and deep: An ideotype to optimize water and n acquisition by maize root systems. *Annals of botany*, *112*(2), 347–357.

Lynch, J. P. (2015). Root phenes that reduce the metabolic costs of soil exploration: Opportunities for 21st century agriculture. *Plant, Cell & Environment*, *38*(9), 1775–1784.

Lynch, J. P. (2022). Harnessing root architecture to address global challenges. *The Plant Journal*, *109*(2), 415–431.

Lynch, J. P., Galindo-Castañeda, T., Schneider, H. M., Sidhu, J. S., Rangarajan, H., & York, L. M. (2024). Root phenotypes for improved nitrogen capture. *Plant and Soil*, *502*(1), 31–85.

Mishra, S., Levengood, H., Fan, J., & Zhang, C. (2024). Plants under stress: Exploring physiological and molecular responses to nitrogen and phosphorus deficiency. *Plants*, *13*(22), 3144.

Pagès, L., & Pellerin, S. (1994). Evaluation of parameters describing the root system architecture of field grown maize plants (zea mays l.) ii. density, length, and branching of first-order lateral roots. *Plant and Soil*, *164*(2), 169–176.

Pagès, L., Vercambre, G., Drouet, J.-L., Lecompte, F., Collet, C., & Le Bot, J. (2004). Root typ: A generic model to depict and analyse the root system architecture. *Plant and soil*, *258*(1), 103–119.

Perkins, A. C., & Lynch, J. P. (2021). Increased seminal root number associated with domestication improves nitrogen and phosphorus acquisition in maize seedlings. *Annals of botany*, *128*(4), 453–468.

Postma, J. A., Dathe, A., & Lynch, J. P. (2014). The optimal lateral root branching density for maize depends on nitrogen and phosphorus availability. *Plant physiology*, *166*(2), 590–602.

Prasanna, B., & Sharma, L. (2005). The landraces of maize (zea mays l.): Diversity and utility. *Indian Journal of Plant Genetic Resources*, *18*(02), 155–168.

Rangarajan, H., Hadka, D., Reed, P., & Lynch, J. P. (2022). Multi-objective optimization of root phenotypes for nutrient capture using evolutionary algorithms. *The Plant Journal*, *111*(1), 38–53.

Richardson, K., Steffen, W., Lucht, W., Bendtsen, J., Cornell, S. E., Donges, J. F., Drüke, M., Fetzer, I., Bala, G., Von Bloh, W., et al. (2023). Earth beyond six of nine planetary boundaries. *Science advances*, *9*(37), eadh2458.

Robinson, D. (1994). The responses of plants to non-uniform supplies of nutrients. *New Phytologist*, *127*(4), 635–674.

Schloerke, B., Cook, D., Larmarange, J., Briatte, F., Marbach, M., Thoen, E., Elberg, A., & Crowley, J. (2025). *Ggally: Extension to 'ggplot2'* [R package version 2.4.0]. https://doi.org/10.32614/CRAN.package.GGally

Schneider, H. M., Lor, V. S. N., Hanlon, M. T., Perkins, A., Kaeppler, S. M., Borkar, A. N., Bhosale, R., Zhang, X., Rodriguez, J., Bucksch, A., et al. (2022). Root angle in maize influences nitrogen capture and is regulated by calcineurin b-like protein (cbl)-interacting serine/threonine-protein kinase 15 (zmcipk15). *Plant, Cell & Environment*, *45*(3), 837–853.

Steffen, W., Richardson, K., Rockström, J., Cornell, S. E., Fetzer, I., Bennett, E. M., Biggs, R., Carpenter, S. R., De Vries, W., De Wit, C. A., et al. (2015). Planetary boundaries: Guiding human development on a changing planet. *science*, *347*(6223), 1259855.

Trachsel, S., Kaeppler, S., Brown, K., & Lynch, J. (2013). Maize root growth angles become steeper under low n conditions. *Field Crops Research*, *140*, 18–31.

Villa, T. C. C., Maxted, N., Scholten, M., & Ford-Lloyd, B. (2005). Defining and identifying crop landraces. *Plant genetic resources*, *3*(3), 373–384.

Wang, Q., Li, S., Li, J., & Huang, D. (2024). The utilization and roles of nitrogen in plants. *Forests*, *15*(7), 1191.

Wang, Y., Ying, H., Yin, Y., Zheng, H., & Cui, Z. (2019). Estimating soil nitrate leaching of nitrogen fertilizer from global meta-analysis. *Science of the Total Environment*, *657*, 96–102.

Wei, T., & Simko, V. (2024). *R package 'corrplot': Visualization of a correlation matrix* [(Version 0.95)]. https://github.com/taiyun/corrplot

Wingler, A., Purdy, S., MacLean, J. A., & Pourtau, N. (2006). The role of sugars in integrating environmental signals during the regulation of leaf senescence. *Journal of experimental botany*, *57*(2), 391–399.

Yadav, M., Kumar, R., Parihar, C., Yadav, R., Jat, S., Ram, H., Meena, R., Singh, M., Verma, A., Kumar, U., et al. (2017). Strategies for improving nitrogen use efficiency: A review. *Agricultural Reviews*, *38*(1).

Zayed, O., Hewedy, O. A., Abdelmoteleb, A., Ali, M., Youssef, M. S., Roumia, A. F., Seymour, D., & Yuan, Z.-C. (2023). Nitrogen journey in plants: From uptake to metabolism, stress response, and microbe interaction. *Biomolecules*, *13*(10), 1443.

Zhan, A., & Lynch, J. P. (2015). Reduced frequency of lateral root branching improves n capture from low-n soils in maize. *Journal of Experimental Botany*, *66*(7), 2055–2065.

Zhang, J., Liu, Y., Zhang, S., Zeng, H., Ding, W., Zhang, D., & Xu, G. (2026). Plant nitrogen nutrition: Enhancing plant resilience to abiotic stresses. *Journal of Genetics and Genomics*.

Zhang, X., Davidson, E. A., Mauzerall, D. L., Searchinger, T. D., Dumas, P., & Shen, Y. (2015). Managing nitrogen for sustainable development. *Nature*, *528*(7580), 51–59.

Zobel, R., & Waisel, Y. (2010). A plant root system architectural taxonomy: A framework for root nomenclature. *Plant Biosystems*, *144*(2), 507–512.

Appendices

A. Seed disinfection and germination

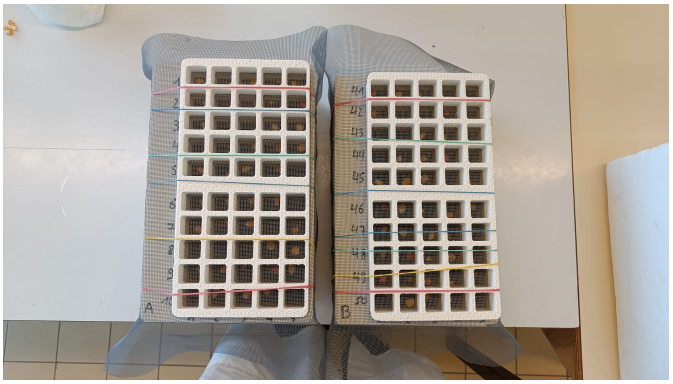

Figure A.1: Seed disinfection step before germination. Seeds were disinfected before being placed under germination conditions.

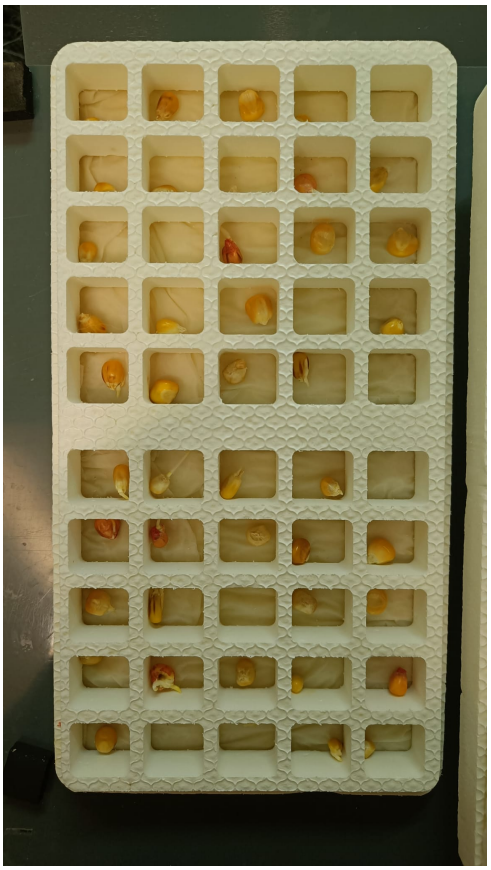

Figure A.2: Germinated maize seedlings before transfer to the RootPhAir platform.

B. Temperature and humidity during the experiments

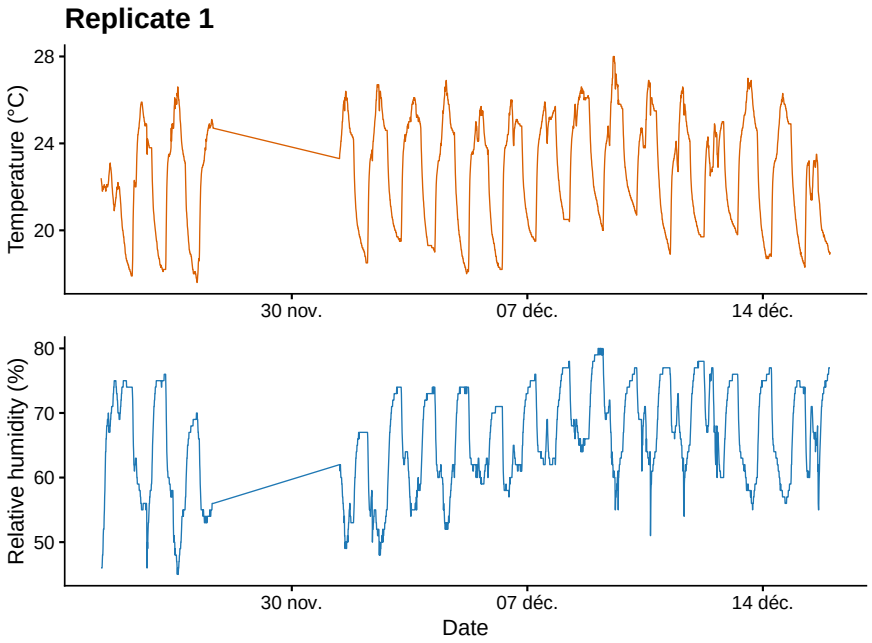

(a) Experiment 1

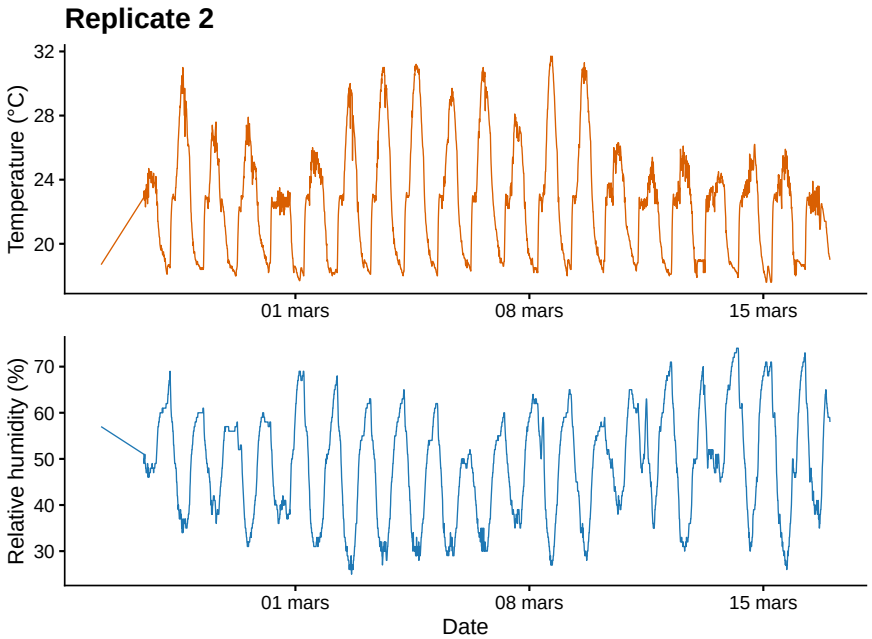

(b) Experiment 2

Figure A.3: Evolution of temperature and relative humidity during the two main experiments conducted in the greenhouse.

C. Seed holders used on the RootPhAir platform

(a) Standard seed holders.

(b) Seed holder at the end of the experiment.

Figure A.4: Types of holders used to maintain maize seedlings on the RootPhAir platform during the experiments.

D. Detailed composition of the nutrient solutions

Table A.1: Solution 1 — 6 mmol/L of N

Reagents		**Stock solution**		**Final solution**		
Components	**M.W. (g/mol)**	**[C] (Mol/L)**	**[C] (g/L)**	**V(mL) for 1L**	**V(mL) for 25L**	**Final [C]**
KNO_3	101.103	2	202	0	0	0
K_2SO_4	174.259	0.5	87	5	125	0.0025
$Ca(NO_3)_2$ x $4H_2O$	236.15	2	472	1.324	33.088	0.003
$MgSO_4$ x $7H_2O$	246.47	2	493	1	25	0.002
NH_4NO_3	80.04	1	80	0.353	8.824	0.0004
Components	**M.W. (g/mol)**	**[C] (Mol/L)**	**[C] (g/L)**	**m(g) for 1L**	**m(g) for 25L**	**Final [C]**
$CaSO_4$ x $2H_2O$	172.172	/	/	0.405110588	10.12776471	0.002352941

Table A.2: Solution 2 — 3 mmol/L of N

Reagents		**Stock solution**		**Final solution**		
Components	**M.W. (g/mol)**	**[C] (Mol/L)**	**[C] (g/L)**	**V(mL) for 1L**	**V(mL) for 25L**	**Final [C]**
KNO_3	101.103	2	202	0	0	0
K_2SO_4	174.259	0.5	87	5	125	0.0025
$Ca(NO_3)_2$ x $4H_2O$	236.15	2	472	0.662	16.544	0.001
$MgSO_4$ x $7H_2O$	246.47	2	493	1	25	0.002
NH_4NO_3	80.04	1	80	0.176	4.412	0.0002
Components	**M.W. (g/mol)**	**[C] (Mol/L)**	**[C] (g/L)**	**m(g) for 1L**	**m(g) for 25L**	**Final [C]**
$CaSO_4$ x $2H_2O$	172.172	/	/	0.632985294	15.82463235	0.003676471

Table A.3: Solution 3 — 1.5 mmol/L of N

Reagents		**Stock solution**		**Final solution**		
Components	**M.W. (g/mol)**	**[C] (Mol/L)**	**[C] (g/L)**	**V(mL) for 1L**	**V(mL) for 25L**	**Final [C]**
KNO_3	101.103	2	202	0	0	0
K_2SO_4	174.259	0.5	87	5	125	0.0025
$Ca(NO_3)_2$ x $4H_2O$	236.15	2	472	0.331	8.272	0.001
$MgSO_4$ x $7H_2O$	246.47	2	493	1	25	0.002
NH_4NO_3	80.04	1	80	0.088	2.206	0.0001
Components	**M.W. (g/mol)**	**[C] (Mol/L)**	**[C] (g/L)**	**m(g) for 1L**	**m(g) for 25L**	**Final [C]**
$CaSO_4$ x $2H_2O$	172.172	/	/	0.746922647	18.67306618	0.004338235

Table A.4: Solution 4 — 1 mmol/L of N

Reagents		**Stock solution**		**Final solution**		
Components	**M.W. (g/mol)**	**[C] (Mol/L)**	**[C] (g/L)**	**V(mL) for 1L**	**V(mL) for 25L**	**Final [C]**
KNO_3	101.103	2	202	0	0	0
K_2SO_4	174.259	0.5	87	5	125	0.0025
$Ca(NO_3)_2$ x $4H_2O$	236.15	2	472	0.221	5.515	0.000
$MgSO_4$ x $7H_2O$	246.47	2	493	1	25	0.002
NH_4NO_3	80.04	1	80	0.059	1.471	0.0001
Components	**M.W. (g/mol)**	**[C] (Mol/L)**	**[C] (g/L)**	**m(g) for 1L**	**m(g) for 25L**	**Final [C]**
$CaSO_4$ x $2H_2O$	172.172	/	/	0.784901765	19.62254412	0.004558824

Table A.5: Solution 5 — 0.5 mmol/L of N

Reagents		**Stock solution**		**Final solution**		
Components	**M.W. (g/mol)**	**[C] (Mol/L)**	**[C] (g/L)**	**V(mL) for 1L**	**V(mL) for 25L**	**Final [C]**
KNO_3	101.103	2	202	0	0	0
K_2SO_4	174.259	0.5	87	5	125	0.0025
$Ca(NO_3)_2$ x $4H_2O$	236.15	2	472	0.110	2.757	0.000
$MgSO_4$ x $7H_2O$	246.47	2	493	1	25	0.002
NH_4NO_3	80.04	1	80	0.029	0.735	0.0000
Components	**M.W. (g/mol)**	**[C] (Mol/L)**	**[C] (g/L)**	**m(g) for 1L**	**m(g) for 25L**	**Final [C]**
$CaSO_4$ x $2H_2O$	172.172	/	/	0.823	20.572	0.005

Minor elements were added at constant concentrations for all nutrient solutions, independently of the nitrogen level.

Table A.6: Composition of minor elements (independent of nitrogen concentration)

Reagents		**Stock solution**		**Final solution**		
Components	**M.W. (g/mol)**	**[C] (Mol/L)**	**[C] (g/L)**	**V(mL) for 1L**	**V(mL) for 25L**	**Final [C]**
Minor elements:						
H_3BO_3	61.83	0.0463	2.86			0.000046
$MnCl_2$ x $4H_2O$	197.91	0.0091	1.81			0.000091
$ZnSO_4$ x $7H_2O$	287.56	0.0008	0.22	1	25	7.6E-07
$CuSO_4$ x $5H_2O$	249.69	0.0002	0.051			3.1E-07
H_3MoO_4 x H_2O	180.97	0.0005	0.09			4.9E-07
KH_2PO_4	136.08	1	136	0.5	12.5	0.0005
$C_{10}H_{12}N_2FeNaO_8$	421.1	0.0356	15	3	75	0.0001068

E. Visual observations during the experiments

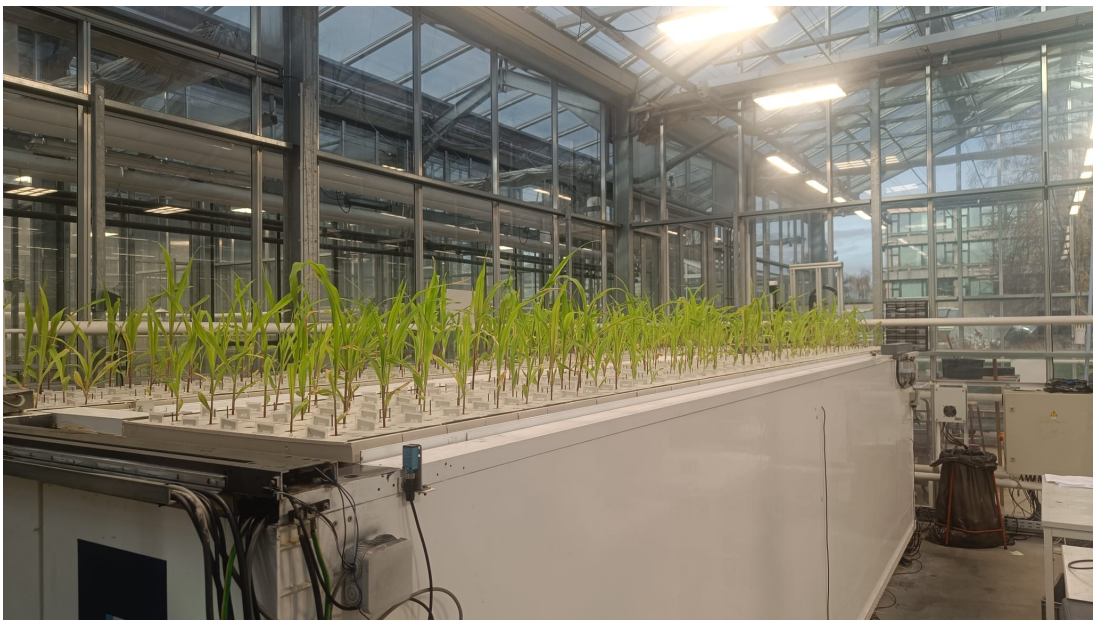

Figure A.5: Aboveground parts of maize plants after 15 days of growth under low nitrogen conditions, corresponding to 0.5 mmol L^{-1} of nitrogen.

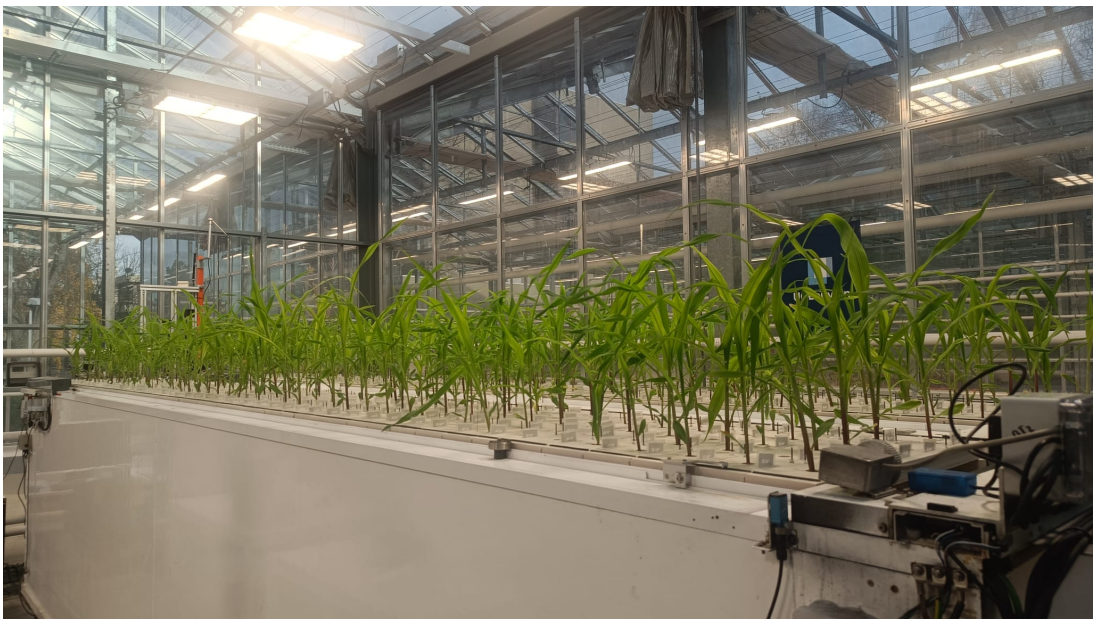

Figure A.6: Aboveground parts of maize plants after 15 days of growth under moderate nitrogen conditions, corresponding to 3 mmol L^{-1} of nitrogen.

Figure A.7: Maize root systems growing in the aeroponic system during the first replicate of the second experiment.

F. Confidence codes used during angle measurements

Table A.7: Confidence codes used to identify anomalies observed during root angle measurements.

Code	Description
1	Very unstable lateral roots
2	Presence of two roots, but the lateral root was still measurable
3	Large number of seminal roots present from the beginning
4	A neighbouring plant grew underneath the observed root system
5	A neighbouring plant fell underneath the observed root system
6	Witch's broom phenotype
7	Neighbouring plant growing underneath, or extremely large neighbouring root
8	Strong lateral growth of the primary root
9	Stem growth failure
10	Severe drought impact causing root growth arrest

G. Specific annotations used in image analysis

Table A.8: Annotation codes used during Aerogrow image analysis.

Code	Description
na	No growth or dead plant
nb	Presence of a neighbouring root
wb	Witch's broom phenotype
sst	Seminal roots stuck together
hs	Water-deficit event
large	Seminal root tip too large to measure
dif	Difference in lateral root density
delay	Delayed growth
nodpd	No DPD measurement
slowdown	Unstable root growth
ok	No abnormality detected
petite	Abnormally small plant
nospeed	Unable to measure root growth speed

H. Candidate mixed models

Several linear mixed-effects model structures were evaluated for each trait. Models differed in the inclusion of experimental tank, spatial block effects and plant age. The fixed-effects structure was identical across models and included variety group, variety nested within group, nitrogen treatment and their interactions.

Table A.9: Candidate mixed models evaluated during model selection.

Model	Structure
Mix1	*group* + *ENTRYCODE(group)* + *N_treatment* $+$*group* $\times$ *N_treatment* $+$*ENTRYCODE(group)* $\times$ *N_treatment*
Mix2	Mix1 $+$*EXP_TANK*
Mix3	Mix2 $+(1\|$*EXP_TANK:ROWBLOCK*$)$
Mix4	Mix3 $+(1\|$*EXP_TANK:COLBLOCK*$)$
Mix1A	Mix1 $+(1\|$*AGE_c*$)$
Mix2A	Mix2 $+(1\|$*AGE_c*$)$
Mix3A	Mix3 $+(1\|$*AGE_c*$)$
Mix4A	Mix4 $+(1\|$*AGE_c*$)$

I. Principal component analyses of trait values under contrasting nitrogen treatments

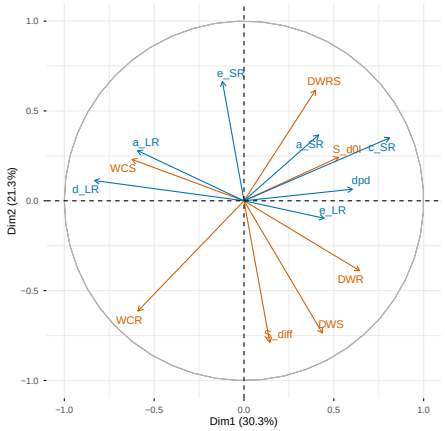

(a) Correlation circle under severe low nitrogen (0.5 mM N).

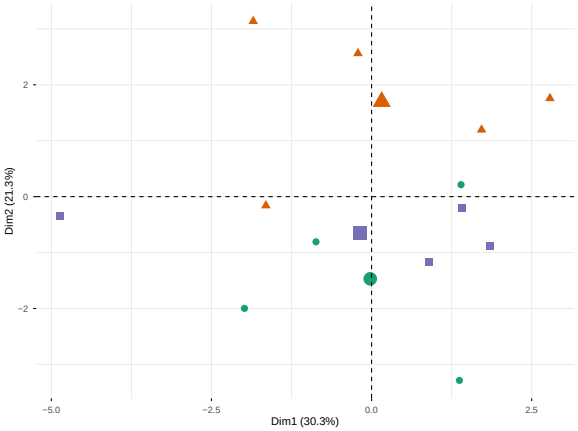

(b) Individual factor map under severe low nitrogen (0.5 mM N).

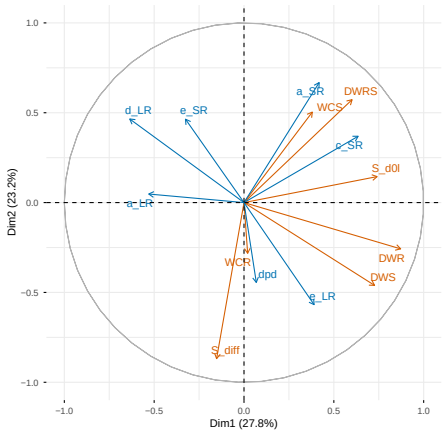

(c) Correlation circle under moderate low nitrogen (3 mM N).

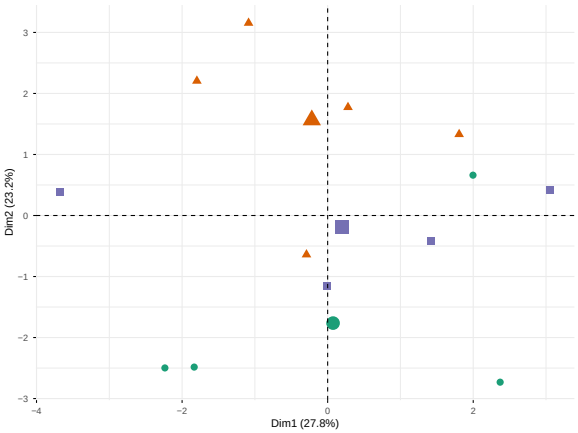

(d) Individual factor map under moderate low nitrogen (3 mM N).

Figure A.8: Principal component analyses (PCA) performed using the 14 phenotypic traits measured under severe low nitrogen (0.5 mM N) and moderate low nitrogen (3 mM N). Correlation circles (A, C) display the contribution and relationships among variables, whereas individual factor maps (B, D) show the distribution of genotypes on the first two principal components. In the individual factor maps, colours indicate genotype groups: hybrids (orange), high-efficiency landraces (green) and low-efficiency landraces (blue). In the correlation circles, root system architecture traits are shown in blue and biomass and physiological traits are shown in orange.

J. Replicate effect on seminal root elongation rate

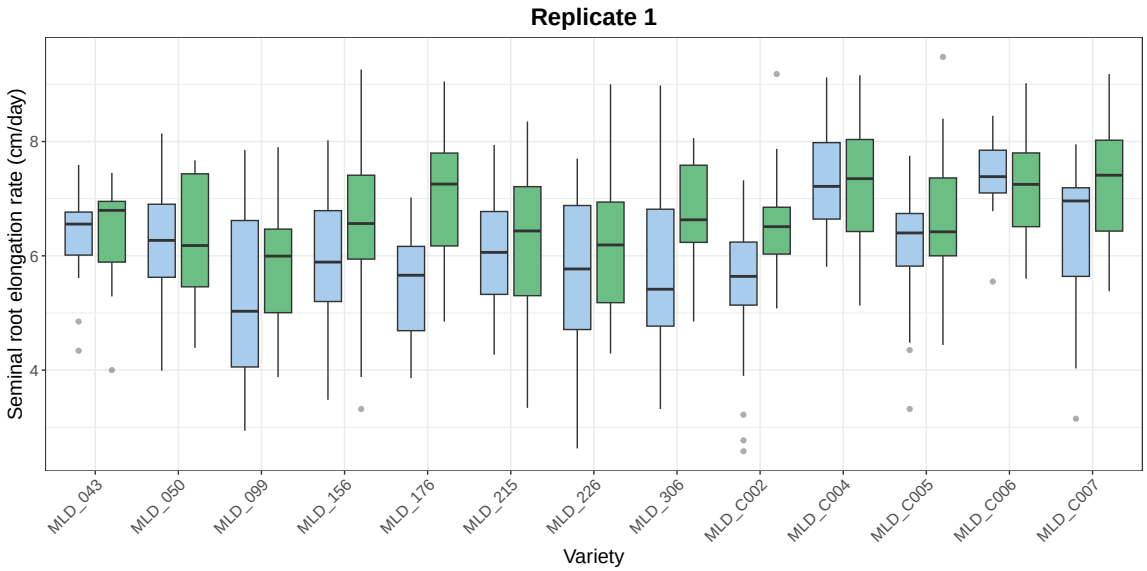

(a)

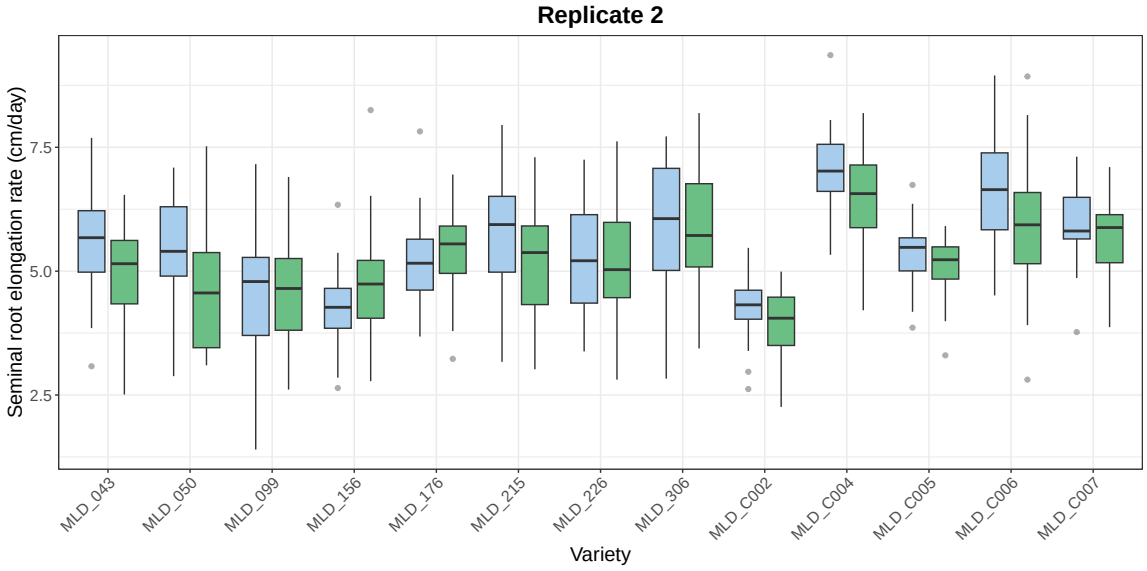

(b)

Figure A.9: Distribution of seminal root elongation rate ($erate_c m_d$) across maize genotypes under the two nitrogen treatments in Replicate 1 (A) and Replicate 2 (B). Blue boxplots correspond to severe low nitrogen (0.5 mM N) and green boxplots to moderate low nitrogen (3 mM N). The figure illustrates the marked experiment effect observed for this trait, which was likely influenced by the temporary irrigation failure that occurred during Replicate 2.

K. Timing of seminal root angle measurements

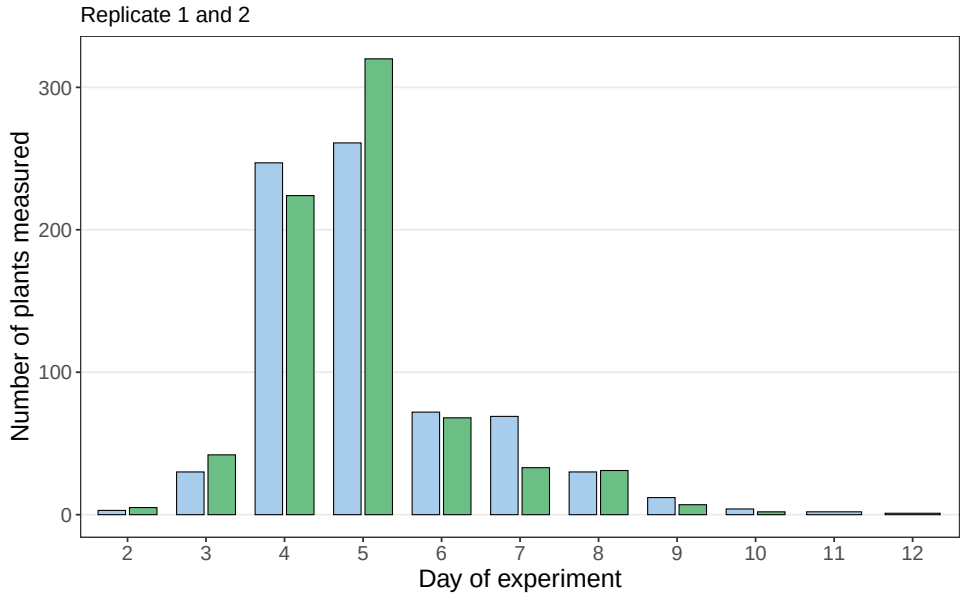

Figure A.10: Distribution of the dates at which seminal root angle measurements were performed. For each plant, the angle was measured on the last image acquired before the emergence of lateral roots, ensuring that measurements were taken at a comparable developmental stage. The figure shows the number of plants measured according to the number of days elapsed since germination.

Root system architecture of contrasted maize landraces under nitrogen deficit

Emilie Devaux

ABSTRACT

Nitrogen (N) is a critical limiting nutrient in crop production, and improving nitrogen use efficiency (NUE) in maize represents a major challenge for sustainable agriculture. Root system architecture (RSA) plays a central role in N acquisition, as it determines the plant's capacity to explore the soil and access spatially heterogeneous N resources. This study investigated how contrasting N conditions affect root architectural and biomass-related traits in a panel of 13 maize varieties, including eight European landraces classified as high or low NUE, and five hybrid varieties.

Plants were grown on the aeroponic RootPhAir platform under two N treatments severe low N (0.5 mM) and moderate low N (3 mM) over a three-week period. Root traits including seminal root (SR) angle, lateral root (LR) angle, LR density, elongation rates, and duration of primordium development were measured using dedicated image analysis software. Biomass and physiological traits were assessed at harvest.

N limitation strongly reduced shoot and root biomass, with shoot dry weight decreasing by approximately 60% and root dry weight by 35%, resulting in a marked increase in the root-to-shoot ratio. In contrast, most root architectural traits showed limited plastic responses to N availability. LR density and elongation rate were reduced under severe N limitation, suggesting resource conservation rather than enhanced soil exploration. No consistent effect of N treatment was observed on SR elongation rate, possibly due to confounding effects of a water stress event during the second replicate.

Multivariate analyses revealed coordinated plastic responses among biomass traits, and a negative association between LR density plasticity and root elongation plasticity, suggesting a resource allocation trade-off. Contrary to initial expectations, high- and low-NUE landraces could not be clearly distinguished based on early root traits, indicating that NUE differences may manifest at later developmental stages or depend on physiological mechanisms not captured here.

Overall, the results suggest that adaptation to N limitation in young maize plants involves coordinated adjustments across multiple traits rather than strong modifications of individual architectural characteristics, and that genotypic variation in plasticity is more prominent within predefined NUE groups than between them.

Université catholique de Louvain
Faculté des bioingénieurs
Croix du Sud, 2bte L7.05.01, 1348 Louvain-La-Neuve, Belgique | www.uclouvain.be/agro